Radial growth decline in a tropical Andean treeline in Bolivia

Rose Oelkers[1,2], Laia Andreu-Hayles[1,3,4], Rosanne D'Arrigo[1], Hung T. T. Nguyen[2], Arturo Pacheco Solana[2,5], Milagros Rodriguez-Caton[2,6], M. Eugenia Ferrero[6,11], Ernesto Tejedor[7], Alfredo F. Fuentes[8,9], Carla Maldonado[8,9], Daniel Ruiz-Carrascal[10]

[1]Lamont-Doherty Earth Observatory of Columbia University, Palisades, NY 10964, USA
[2]Department of Earth Science and Environmental Change, University of Illinois Urbana-Champaign, Urbana, IL, USA
[3]Ecological and Forestry Applications Research Center (CREAF), Bellaterra, Spain
[4]Catalan Institution for Research and Advanced Studies (ICREA), Barcelona, Spain
[5]Department of Land, Environment, Agriculture and Forestry (TeSAF), University of Padua, 35020 Legnaro, Italy
[6]Instituto Argentino de Nivología, Glaciología y Cs. Ambientales (IANIGLA), CONICET Mendoza, Argentina
[7]Department of Geology, National Museum of Natural Sciences-Spanish National Research Council (MNCN-CSIC), Madrid. Spain
[8]Herbario Nacional de Bolivia, Instituto de Ecología, Carrera de Biología, Facultad de Ciencias Puras y Naturales, Universidad Mayor de San Andrés, La Paz, Bolivia
[9]Latin America Department, Science & Conservation Division, Missouri Botanical Garden, St. Louis, MO, USA
[10]Innovation and Technological Development Directorate, Universidad EAFIT, Medellin, Colombia
[11]Laboratorio de Dendrocronología, Universidad Continental, Huancayo, Peru

Correspondence to: Rose Oelkers roelkers@ldeo.columbia.edu; rco19@illinois.edu

Abstract. The impacts of rising temperatures in tropical treeline ecosystems remains understudied. Here we report on a remarkable decline in the radial growth of *Polylepis pepei* BB.Simpson, a tropical tree species that grows in a monospecific forest at the elevational treeline in the Andes-Amazon ecotone of Bolivia. Using dendrochronological methods we developed an annually resolved tree-ring width chronology spanning from 1850 to 2018 C.E. To our knowledge this is the longest record of annual tree-growth (169 yrs) for this species. This chronology revealed a significant ($p = 0.01$) radial growth decline in *P. pepei* after 1997, which was also observed in other high-elevation *Polylepis* forests of tropical South America (> 17° S; 4600 m a.s.l.). Between 1960-2015, *P. pepei* RW was mostly regulated by prior-year minimum temperature and mean precipitation variability during the wet season (~November-March). RW-climate correlations suggest the observed growth decline at this tropical treeline is likely due to temperature driven moisture stresses. Smaller ring-width was associated with drier and warmer conditions in the forest while wetter and cooler conditions led to enhanced growth in the following year. Between 1960-2015, minimum temperature significantly increased during the wet season, while precipitation decreased. These climate trends observed in our study region in the Madidi National Park may indicate a reduction in moisture convergence and transport to higher elevations where our forest is located. If temperature continues to rise at current rates, one of the highest-elevation tree species on the globe, *P. pepei*, could face severe consequences.

1 Introduction

The stability of tropical Andean treeline communties under global warming has become of great concern due to observed shifts in forest composition, distribution and increased tree mortality in recent decades (Cuesta et al., 2020; Feeley et al., 2012, 2011; Macek et al., 2009; Young and León, 2006). In South America, forests found near the mountain peaks in the Andes Mountains are often referred to as 'treeline' or high mountain areas in literature (Hock et al., 2019; Körner, 2012; Young and León, 2006) and the term used herein is used to describe the upper range limits of the tree species found in the region. Plot studies in the Peruvian Andes-Amazon found that the position of Andean timberline (i.e. elevational limit of closed-canopy forests) is limited by seed dispersal (Rehm and Feeley, 2013). Dendrochronology has been widely used to evaluate annual growth variability and long-term climate response of treeline forests in the northern Hemisphere (Büntgen et al., 2022; D'Arrigo et al., 1999; MacDonald et al., 2007). However, tropical tree-ring studies in South America (~8°N-24°S), are noticeably scarce in comparison to higher latitude regions (Andreu-Hayles et al., 2023; Groenendijk et al., 2025; Quesada-Román et al., 2022). Still, some relevant studies have provided key understanding of climate-growth response of high elevation forests in the tropical Andes as described below.

A study from the Peruvian puna (upper Andes) presented the first tree-ring chronology of *Escallonia myrtilloides* L.phil. (Requena-Rojas et al., 2021), a species often found at tropical treeline (Zapata, 2013), in which the authors showed radial growth is positively correlated to precipitation, and negatively correlated to temperature variability in this region. In the central Andes of Peru, *Requena-Rojas* et al. (2020) analyzed the tree rings from three *Polylepis* species, and found these trees are slow-growing and sensitive to both current-year temperature and prior year precipitation changes. In subtropical regions, prior-year moisture availability was the dominant limiting factor for *Polylepis tarapacana* Phil. treelines in Argentina, based on RW-climate correlations spanning 1934-1980 (Morales et al. 2004) On the other hand, the growth of several tropical montane species in northern Argentina appears to be regulated only by temperature at the upper elevations of an altitudinal gradient (Ferrero et al., 2013). Although seedling recruitment of *Northfagus pomillo* is driven by temperature variability, the rate of seedling establishment was limited by overall moisture conditions in Patagonia (Srur et al., 2018, 2016). Yet, there was a radial growth decline in *Nothofagus pumilio* at a Chilean treeline site, where precipitation had increased (Álvarez et al., 2015), possibly suggesting a non-linear growth response of these forests to climate.

Here we describe a tropical treeline site of *Polylepis pepei* BB.Simpson (Simpson, 1979), growing high elevations (3800 - 4000 m.a.s.l.) in the Andes-Amazon corridor of Bolivia in South America. This site is located at upper forested limit of Bolivia's Madidi National Park (MNP), a hotspot for biodiversity just east of the Cordillera Real in the Andes Temperature and humidity gradients shape unique ecotones in the *MNP* including diverse seasonally dry forests near the Tuichi River (~850 m.a.s.l.) and humid monospecifc forests at Andean treeline (~4400 m.a.s.l.).─The hydroclimate of the MNP (and Andes-Amazon) is primarily influenced by the South American Summer Monsoon (SASM), which peaks in the tropics during austral

summer (December-February). Inter-annual to decadal sea surface temperature sea-surface temperature (SST) conditions in the Pacific and Atlantic Oceans also impact climate in the region (Paegle and Mo, 2002; Vuille et al., 2000). Originating in the tropical Pacific, the El Niño Southern Oscillation (ENSO) system is the dominant mode of annual to decadal hydroclimate variability in South America and indeed the globe (e.g. Garreaud, 2009; Vera et al., 2006; Vuille et al., 2000). ENSO-related anomalies SST anomalies have contributed to extreme weather events in South America such as seasonal drought, flooding, and other geohazards (Vera et al., 2006; Vuille et al., 2000). Tree-ring width and oxygen isotopes have recorded these exteme events at treeline *P. tarapacana* in the central tropical Andes and provided year-to-year to centennial records of ENSO variability overall(Christie et al., 2009; Crispín-DelaCruz et al., 2022; Rodriguez-Caton et al., 2022) Currently there is no information on the impacts of such ENSO-related climate extremes on *Polylepis pepei* tree-rings, or for treeline sites within the MNP.

The geographic range of *Polylepis pepei* (family Rosaceae; common name "Kenua" or "Queñoa") spans from central Bolivia to northern Peru (Simpson, 1979) between 3550-4800 m.a.s.l. (Espinoza and Kessler, 2022). Tree-ring studies in Bolivian and Peru have shown *P. pepei* can reach significant age (>135 years) and the RW can be sensitive to prior and current-year climate variability (Jomelli et al., 2012; Roig et al., 2001).The wide dispersion of leaves along the branches in *P. pepei* and its long fruit distinguish this species from other *Polylepis* spp. The genus name *Polylepis* is derived from the Greek words 'many layers', describing multiple layers of compressed thin-bark sheets, a functional trait that allows these trees to survive freezing air temperatures. This species is also adapted to cold soil temperatures in the eastern cordillera of the Andes. Ecological studies of *P. pepei* sites between 3800~4300 m.a.s.l. in Peru (Kessler et al., 2014) and Bolivia (Hoch and Körner, 2005) recorded (> 5cm) soil temperatures ranging from 3-5°C during the wet season.

Like much of the treeline species across the Andes-Amazon, *P. pepei* is under threat of shifting temperature regimes and human impacts on the ecosystem. Some studies predict the germination and spatial distribution of treeline *Polylepis spp* in the Andes is projected to decrease as vapor pressure deficits, temperatures, and overall aridity increase (Cuyckens et al., 2016; López et al., 2022). Southwest of our *P. pepei* site, in the central Andes of southern Peru ice proxy data indicated recent surface warming in the tropics that appears unprecedented in 5000 years (Thompson et al., 2006). In November 2009 temperatures were so warm that a catastrophic glacial lake outburst flood eliminated roads, livestock, and structures in the small community of Keara Bolivia (< 3800 m.a.s.l.; Hoffmann and Weggenmann, 2013). In the MNP, there is evidence of a temperature-induced migration (i.e. thermophilization) of mid-elevation tree species towards Andes ecotones caused by increased of tree mortality near the treeline (Farfan-Rios et al. 2025).

Humans also play a role in modifying the forested landscape near the MNP. Ilegal mining and logging activities in low-elevation forests (<1200 m.a.s.l.) have deteriorated forest structure and health, with increasing loss of forest cover in recent years (Finer and Mamani, 2023). Prior to the designation of Madidi as a National Park in 1995, large swaths of economically-

valuable trees along riverbanks (e.g. *Amburana cearensis* Smith) were harvested for timber (Macía, 2008). Today, *P. pepei* is at great risk of endangerment due to habitat loss related to fires and land conversion for cattle ranching or religious practices (Espinoza and Kessler, 2022; Kessler et al., 2014). These losses of primary forests have severe implications for carbon storage capacity, ecosystem function, and land stability, all critical factors for the survival of native inhabitants. Herein, efforts were made to minimize potential impacts of land use and disturbance in field sampling, but ecosystem disturbances in certain regions of the MNP were nevertheless observed. Since this ecotone is facing a rapidly changing environment due to climate and human-related disturbances, high resolution tree-ring records at this treeline may offer valuable insight on past and current growth responses.

At present, only two tree-ring studies have been published for the MNP: one for *Juglans boliviana* (C.DC.) Dode (14°40' S, 68°41' W; 1300 m.a.s.l.) in *Oelkers* et al. (2023) and another by *Andreu-Hayles* et al. (2015), the latter confirming the formation of annual rings in a *Pseudomedia rigida* (Klotzsch & H.Karst.) Cuatrec. cross-section (14°33′S, 68°49′W; 1000 m.a.s.l). The *Polylepis pepei* site investigated for this study is found between ~3800-4400 m.a.s.l. in the western MNP (14°40′-14°43′S; 69°04′-69°06′W). Located near the small settlement of Keara, the vegetation is characterized as Alto-Andino Yungueño (Upper Andean Yungas) forest (Navarro et al., 2010) with a seasonally humid climate. This study area was chosen in part because inventory plots already exist at this location, established by botanists from the National Herbarium in La Paz (Bolivia) and the Missouri Botanical Garden (USA). Our specific objective are: i.) to generate a new RW chronology for *P. pepei*, ii.) to identify the climate variables (*e.g.* mean temperature, precipitation, drought), that are the most limiting for annual growth and iii.) to assess the impacts of extreme climate events on the RW variations.

2 Materials and Methods

2.1 Site description and climatology

Our study site is located in northwestern Bolivia (Fig. 1A), where two locations were visited in October 2012 and July 2019 to extract samples of *P. pepei* trees at altitudinal treeline in Keara (Fig. 1C, D). Two to four core samples were extracted from living trees using 2-threaded increment borers (5 mm in diameter). Cross sections of recently dead trees were sliced using a gas-powered chainsaw or a standard saw-tooth blade. In 2019, diameter at breast height (DBH; ~1.2 m) was measured for the trees at the same level that core samples were extracted.

The 2012 collection was from an open-canopy south-facing forest (3795~4100 m.a.s.l.), while the 2019 collection was primarily focused in a closed-canopy west-facing stand in a high-elevation valley called Waca-cocha (named after a nearby lagoon; 4000-4400 m.a.s.l.; Fig. 1D). Both sites feature seasonally humid, upper-montane forests, with persistent mist that evaporates during the day. The sites were largely monospecific, dominated by fragmented patches of *P. pepei* and small

numbners of *Gynoxys compressissima* Cuatrec. trees. Based on field observations in July 2019, the foliage of *P. pepei* may be considered evergreen and the bark consists of thick layers of compressed flakes that are red and brown in color, characteristic of the genus (Appendix A: Fig. A2A). The trees are shrublike, with twisted (and at times, multiple) stems.

The climatology of the study site (1960-2015 Figs. 1B, A1) shows a distinct wet season from October-April and a dry season from June-August (1960-2015; Fig. 1B). The wet season is defined by heavy rainfall (~1900 mm in January; Pre), and warmer mean (6°; Tavg) and maximum temperatures (Tmax; 12-14.7°C). In contrast, the dry season is characterized by low precipitation (65 to 115 mm per month) and extremely cold temperatures (minimum temperature range -7.1 to -8.3°C; Fig A1). Consistent with these patterns the mean diurnal temperature range (the difference between Tmax and Tmin, DTR; Fig A1 B.) is smallest during the peak wet season (12.1 to 16.9°C) due to warmer minimum temperatures (~0°C), and highest during the drier months. Wet-season precipitation and temperature (Oct-Apr) was significantly and negatively correlated between 1960-2015 (r=-0.27, p=0.05) indicating wetter months at this site are typically associated with cooler temperatures, while no significant correlations were found during the dry season.

2.2 Climate data

In this study, we used local precipitation data, and gridded temperature products to generate monthly climate indices near Keara (1960-2015; Fig. 1B). Daily precipitation from the Italaque station in Bolivia (15.48°S, 69.03°W, 3500 m.a.s.l.) was gap filled and homogenized to generate a continuous monthly timeseries (Pre) from 1960-2015 following procedures described in *Huerta* et al. (2025a) and the 'redprecc' package in *R* (Huerta et al. 2025b). Raw (daily) precipitation data for Italaque (1978-2005) and nearby stations (~1945-2015, non-continuous) can be obtained from the DECADE dataset (Hunziker et al. 2018), which were originally sourced from the National Meteorology and Hydrology Service of Boliva (SENAMHI; https://senamhi.gob.bo/index.php). Monthly mean (Tavg), minimum (Tmin), maximum (Tmax) temperature data was obtained from the Climatic research Unit TS 4.08 (CRU; 0.5° resolution; Harris et al. 2020). In addition, we also used CRU monthly diurnal temperature range (DTR; 0.5° resolution; 1901-2015), which represents the difference between Tmax and Tmin, to evaluate temperature variability in the region. The monthly climatology (1960-2015) and long-term variability of DTR (and Tmax and Tmin; 1901-2015) can be found in Appendix A Figs. A1 and A4 (see section 2.5 for more details). Satellite-derived rainfall data from the Climate Hazards Infrared Precipitation with Station group V2.0 (CHIRPS, accessed 2025; Funk et al., 2015) was used for spatial precipitation analyses (see Section 2.5). Although CHIRPS v2.0 is limited to observations after 1981, it has a higher spatial resolution (0.05°) than CRU precipitation (0.5°), which can be more effective for spatial climate-growth analyses in regions with complex topography such as our site in the Andes-Amazon.

In August 2011 (one year before the 2012 sampling campaign), HOBO® temperature and relative humidity data loggers (https://www.onsetcomp.com/) were installed near the *P. pepei* trees at 14°40'S 69°06'W (4158 m.a.s.l.) and data was recorded hourly from 1 September 2011 to 2 September 2014. New HOBO sensors were installed in 2021 and collected during fieldwork

in 2023. Unfortunately, the 2021 system batteries failed within 9 months of the launch, and data was limited to only 20 September 2021 to 23 May 2022. Daily minimum, maximum and mean temperature and relative humidity were calculated from 20 September to 23 May (245 days) for the 2011-2012, 2012- 2013, 2013-2014 and 2021-2022 periods (see Appendix A Fig. A3. Kernel density estimates were used to generate and compare probability distributions among the daily time series. Nonparametric Kolmogorov-Smirnov (KS) tests (Kolmogorov, 1933; Smirnov, 1948) were conducted to determine the significance of the mean difference between the daily timeseries. Kernel density and KS tests were conducted using seaborn (Waskom, 2021) and SciPy (Virtanen et al., 2020) packages in *python*.

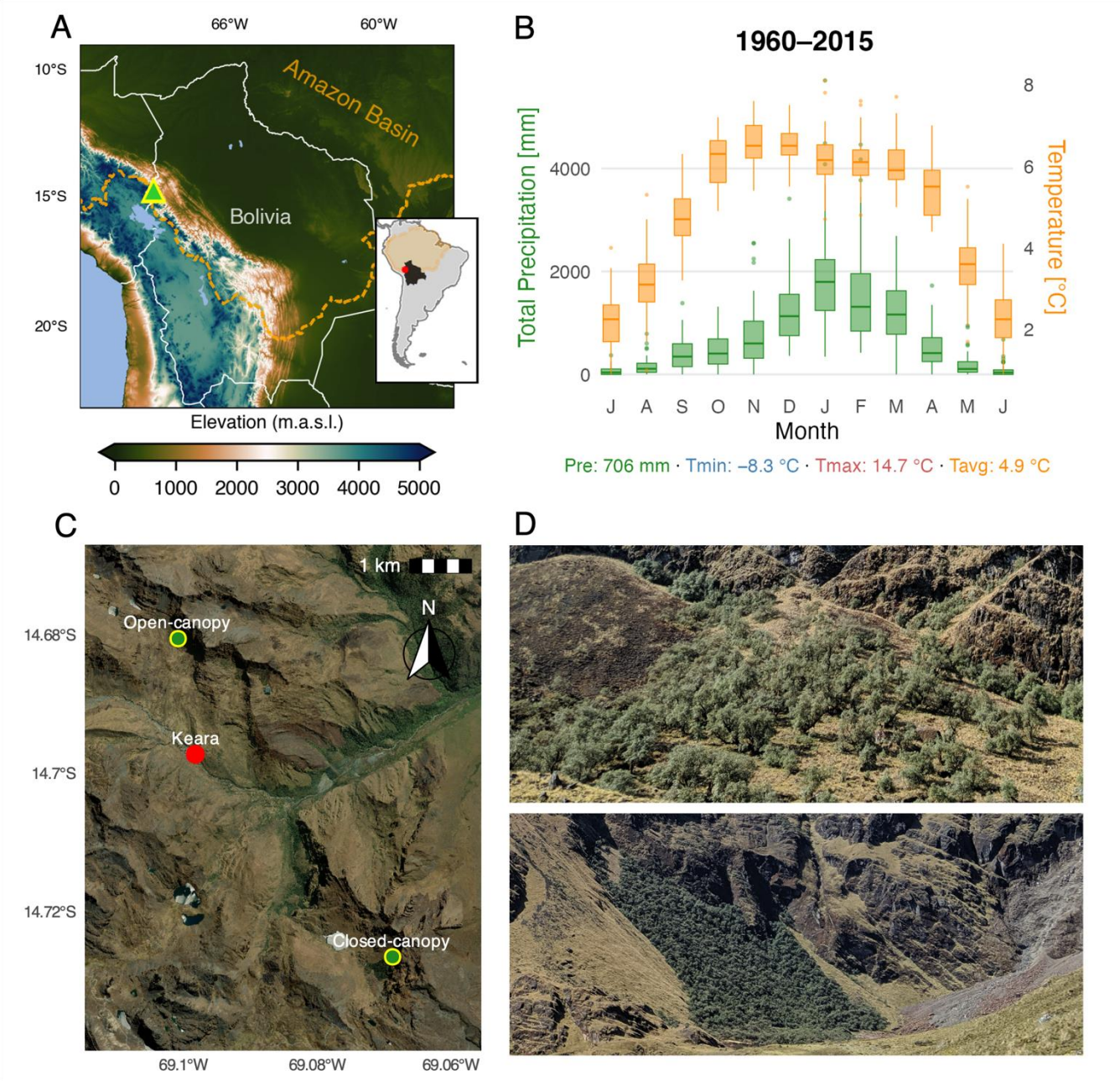

Figure 1: (A) Location of *Polylepis* site in the Eastern Cordillera of the Andes-Amazon ecotone in Bolivia. The orange dotted line (and orange shading in the inset map) represent the spatial limits of the Amazon Basin. The elevation map was generated using the "ETOPO-1" model (https://www.ncei.noaa.gov/products/etopo-global-relief-model; (B) The monthly distribution of mean temperature and total precipitation (1960-2015) in Keara was generated using the nearest temperature CRU gridpoint (14.75°S, 69.5°W) and reconstructed precipitation from the Italaque station (15.48°S, 69.03°W). The average temperature (Tavg), mean precipitation (Pre), and range of minimum and maximum temperatures (Tmin, Tmax) for the study period are included. (C) Aerial view of the sampling locations near the

community of Keara and (D) photos of open-canopy and closed canopy forest patches sampled at altitudinal treeline in Bolivia's MNP (~3700-4400 m.a.s.l.). The basemap in (C) was obtained through opensource ESRI images.

2.3 Wood processing and anatomical analyses

Wood samples were shipped to the Lamont-Doherty Earth Observatory (LDEO) in NY, USA for dendrochronological analysis. Cores and cross sections were finely sanded up to 1000 grit using an orbital sander and manually polished with microfiber paper. Most samples had surficial color differences within the stem, mainly reflecting transitions between the heartwood (functional xylem near the pith, darker color) and sapwood (the active xylem beyond the cambium layer, lighter color).

P. pepei is an angiosperm with diffuse porous wood anatomy, which is typically harder to date than 'ring porous' wood, due to less distinct boundaries between the latewood of the prior year and the earlywood of the current year (Fig. A2). To aid in identifying anatomical properties in the wood, histological (micro) cuts were performed according to techniques described in *von Arx* et al. (2016) using a WSL Core microtome (https://www.wsl.ch/en/services-produkte/microtomes/). *P. pepei* tree rings feature large, semicircular vessel elements in the earlywood that taper tangentially in size towards the transition to latewood, which has thicker, fiber-like tracheid cells (Fig. A2 B).

2.4 Tree-ring chronology development

Tree rings from 51 *P. pepei* samples from 28 living and 3 dead trees (31 trees total) were dated visually using standard dendrochronological techniques (Stokes and Smiley, 1968). RW was measured digitally using the *CooRecorder* image analysis program (Cybis Elektronik, 2010) and statistically crossdated using the program COFECHA (Holmes, 1983) and dplR package in R (Bunn, 2008). To independently confirm annual periodicity of the growth rings, radiocarbon dating was conducted on a cross-section sample (SP20X; Fig. A2) collected in 2019 in the closed-canopy forest. Individual growth rings associated with the years 1957, 1958, 1962, 1963, 1964, 1965, 1971, and 1972 were sliced, extracted for cellulose, and processed for modern radiocarbon analyses. All radiocarbon measurements were compared to the monthly SH $\Delta^{14}C$ radiocarbon curve (1950-2019 C.E.) from the designated atmospheric Zones 1-2 and 3 (SH Zone 1-2; Hua at. 2022). Further details on the radiocarbon analyses and earlier iterations of the Keara RW chronology can be found in the Appendix (Fig. A2 C).

Once final calendar dates were assigned to the tree-ring samples, the Schulman convention (Schulman, 1956), which assigns each ring date to the year growth began, was applied. Individual RW time series were detrended conservatively with age-dependent cubic splines (initial spline stiffness of 60 yrs) (Cook and Peters, 1981; Melvin, 2004). Standardized indices were generated by taking the ratio of the fitted and observed RW values of detrended time series and combined using a robust Tukey bi-weight mean to produce a dimensionless 'standard' RW chronology (Cook et al., 1990). For the residual chronology, autocorrelation was removed from the series using autoregressive modelling determined by the Akaike Information Criterion (Akaike, 1974). The final RW chronologies (standard and residual) represent the entire *P. pepei* RW network (2012 and 2019

tree samples) and thus variance stabilization was applied to account for temporal changes in sample depth (Frank et al., 2006). The standard RW chronology was used for RW-climate correlation analyses, and the residual chronology was used for i.) identification of small or large outliers in the chronology (top 5th and 95th percentiles) and ii.) analyses of the growth response of *P. pepei* to extreme ENSO events (see section 2.6).

The subsample signal strength (SSS) calculation was used to estimate the minimum sample size required to maintain a growth common signal (Wigley et al., 1984). SSS considers the number of cores per tree, the number of individual trees and the mean interseries correlation among RW series to determine how well the available samples reflect the growth signal of the population (i.e. site). An SSS value of 0.85 (or better) is a common threshold in dendrochronology and represents the period when sample size is adequate and the common RW signal is robust (see discussions *Buras* et al., (2017) and *Wigley* et al. (1984) for more details). The Pettit's (1979) changepoint detection test was applied to the raw (radial) RW chronology to detect the timing of recent trends in growth. Significance of the RW trend after the changepoint ($p < 0.05$) was determined by using the non-parametric Mann-Kendall test on the estimated Sen's slope (Sen, 1968) . Changepoint analyses was conducted using the 'trend' package in *R* (Pohlert, 2016).

2.5 Climate-growth analyses

To explore the climate sensitivity of *Polylepis pepei* at the treeline, we correlated annual RW to monthly temperature and precipitation for the period 1960-2015. Monthly temperature data (Tavg, Tmin, Tmax) was from the nearest CRU gridpoint to our site:14.75°S, 69.25°W, while monthly precipitation (Pre) was obtained from local station data (see section 2.2). Monthly Pearson correlations (r) were computed with the stationary bootstrap method implemented with the boot package in R. This technique resamples contiguous blocks of data (n = 1000) at varying block size to preserve autocorrelation and quantify the uncertainty of the RW-climate relationship (see Politis & Romano 1994). Significance of the climate-growth relationship was inferred from the two-tailed 95% confidence intervals (i.e., 95% CI excludes zero). Due to the covariance between temperature and precipitation in this region, we used bootstrapped partial correlations (r_p) to evaluate the independent effect of one variable on RW (e.g. temperature), while controlling for the other (e.g. precipitation). Following methods of *Meko* et al. (2011), partial correlation coefficients for RW-temperature were obtained by: i.) first performing a linear regression between RW and precipitation and ii.) calculating bootstrapped correlations between temperature and the residuals from this regression. The results represent the portion of RW variability not explained by precipitation. Thus, partial correlations show the distinct relationship between RW and temperature while controlling for the influence of precipitation.

Spatial correlations were used to assess the extent of the temperature (Tmax and Tmin) and precipitation signals of the RW within tropical south America. Seasonal climate windows selected for the spatial analyses were inferred from the monthly climate-growth relationships. Spatial correlations with precipitation were conducted using CHIRPS between 1981-2015 (see section 2.2). Otherwise, all monthly and (seasonal) spatial correlation analyses (RW vs. climate) were between 1960-2015.

Field significance was assessed using a binomial test (e.g. the probability *n* number of grid-cell correlations were significant by chance (raw $p<0.05$) due to the high number of comparisons; see: Livezey & Chen, 1983).

Linear trends in the local (seasonal) climate (1960-2015) were assessed using the Sen's slope estimator (section 2.4), and significance was evaluated using Mann Kendall tests. Slopes were reported as the average change in climate in units per decade (Fig. A4) Annual and seasonal (October-April; June-August) trends of diurnal temperature anomalies (DTR) were also evaluated for the same period. Additionally, monthly anomalies of Tmin, and Tmax were calculated relative to the 1901-2015 CRU baseline (full temporal extent of CRU data) to illustrate long-term temperature variability during the wet and dry season (Fig. A5 BC).

2.6 Superposed Epoch Analysis

ENSO varies between warmer (El Niño) and cooler (La Niña) SST phases (Ropelewski and Halpert, 1987) in the Pacific Ocean, and both extremes substantially impact precipitation and temperature conditions over tropical South America. To investigate the effects of extreme ENSO events on tree-growth, Superposed Epoch Analysis (SEA) was performed on the residual RW timeseries (Fig. 2D) using the method originally described by *Haurwitz and Brier* (1981) and modified by *Rao* et al. (2019). SEA is widely used to statistically determine whether the effects of episodic events (e.g. extreme climate events) on a response variable (in this case RW) are statistically significant or due to random noise. The *Rao* method uses 1000 random-sample double bootstrapping to quantify the RW response at the time of the event (lag= 0) and several years after (in this case four years).

We analyzed twenty-six years of RW based on the top-ranked December-February (DJF) El Niño and La Niña events (n=13 each) listed by the National Oceanic and Atmospheric Administration's Physical Science Laboratory (NOAA-PSL: https://psl.noaa.gov/enso/). These ranked DJF years are determined by NOAA-PSL with the multivariate ENSO indices (MEI; 1871~2024). MEI reflects the principal components, or dominant modes, of the entire tropical Pacific ENSO domain (30°N-30°S, 100E°-70°W) rather than any one region (e.g. Niño 3.4) and integrates observations of sea level pressure (SLP), SSTs, meridional (north-south) wind, and outgoing longwave radiation (see Wolter and Timlin, 2011). Extreme years are defined by Pacific SST anomalies during DJF, coincidently when ENSO is phase-locked with the peak monsoon season (Rasmusson and Carpenter, 1982). Annual Pre (station data; 1960-2015) and CRU precipitation and Tavg (nearest gridpoint 1901-2018) were plotted to determine the average climate during years of known ENSO-DJF events near Keara. The list of DJF- ENSO-events obtained from NOAA-PSL are included in Appendix Table A1.

3 Results

3.1 Growth decline in a *P. pepei* tree-ring chronology

The *P. pepei RW* chronology from the MNP treeline spans from 1850-2018 and consists of 51 tree-ring samples (31 trees) from open and closed-canopy forests near Keara (Table 1; Fig. 2). Radiocarbon and standard dendrochronological methods confirmed the growth rings are annual and reflect high frequency patterns of high and low growth through time (Figs. 2A, C, D). Site metadata and chronology statistics for the *P. pepei* network are summarized in Table 1.

Site	Location (elevation)	*n* trees (*n* samples)	Mean age [yrs]	Timespan	Mean RW Correlation	Mean DBH [cm]
Open-canopy forest (south-facing)	14°40'S 69°06'W (3795-4100 m.a.s.l.)	16 living 2 dead (33)	89	1850-2018	0.53	24 cm (*n*=6 trees) *
Closed-canopy forest (west-facing)	14°43'S 69°04W (4000-4400 m.a.s.l.)	12 living 1 dead tree (18)	101	1871-2018	0.44	31 cm
Full network (mean Raw, standard, residual chronologies)	-	31 (51)	93	1850-2018	0.50	30 cm

Table 1. Summary of *P. pepei* tree-ring sample location, age, sample size, and mean correlation of RW timeseries per site. *DBH information is only from the samples collected in 2019 which included 6 trees from the open-canopy forest and 13 trees from the closed-canopy site. The final RW chronologies represent the entire collection of *P. pepei* samples in Keara obtained in both 2012 and 2019.

Due to extreme suppression in radial growth (Fig. 2B), only one or two cores per tree (out of three total) were able to be cross-dated and used for the final RW datasets. A recent decrease in radial growth was observed in samples from both the open-canopy (18 trees) and closed canopy (13 trees) sites (Fig. 2A). The entire Keara *P. pepei* network (mean raw RW; Fig. 2A) has been declining steadily since the 1960s, especially after 1996 ($p = 0.01$), with a less pronounced trend in the standard RW series (Fig. 2AC).

Despite difficulties with crossdating due to suppressed tree-rings, the entire network shared a coherency in the RW patterns with a mean inter-series correlation of $\bar{r} = 0.50$ for the 1850-2018 period (n = 51 samples, 31 trees). The SSS metric indicated the common growth signal was particularly robust (SSS > 0.85) between 1900-2018 when the sample size was greater than 17 (Fig. 2C; average age of the trees 93 yrs). The average radial growth rate between 1850-2018 was 1.04 mm yr^{-1}. DBH measurements in 2019 (6 trees in the open canopy and 13 in the closed-canopy site), confirmed these trees were slow-growing with stem diameters ranging from 10 cm to 54 cm (mean DBH 30 cm).

Years with extremely large RW (95th percentile) included the 1951/52 and 1965/66 growth years (Fig. 2D) which occur before and after a visible growth suppression during the mid-to late 1950s (Fig.2 A, C). Tree rings that began forming in 1906 or 1945 had extremely low values of RW indicating unfavorable growing conditions during the growth-year.

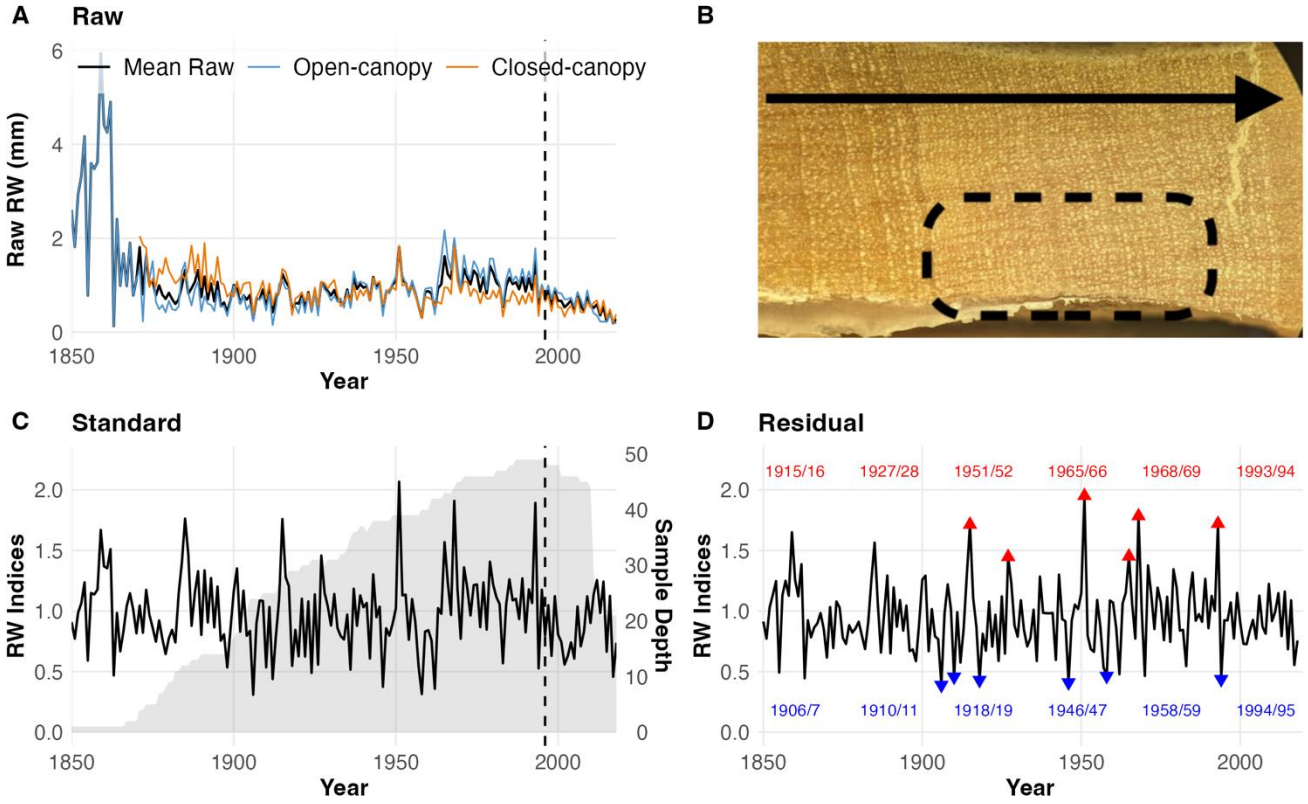

Figure 2. The (A) Raw (C) Standard and (D) Residual RW chronologies of *P. pepei* in Keara. The chronologies (1850-2018) are plotted using the Schulman convention (*i.e.,* anchored on the year of initial ring formation; see section 2.3). (A) There has been a distinct decline in raw (radial) RW since the 1996/1997 growth-year (changepoint is indicated by the black-dotted line. (A) This decline (p=0.01) was evident in both the open-canopy (blue line) and closed-canopy (orange line) forests that were sampled. (B) An image depicts a core sample where several rings are suppressed within a 4 mm distance (dashed circle). The black arrow indicates the direction of radial growth for this core (from left to right). (C) The standard RW is plotted with the mean sample-depth of the full network through time (grey-shading). Triangles on the residual timeseries (D) signify the years within the top 5th (six smallest growth rings; Blue color) and 95th (i.e. largest growth rings; red color) percentiles of RW since 1900 (SSS> 0.85). Since the tree rings are estimated to form during the wet season (two-calendar years ~October-April), both years are labeled in the colored text (ordered chronologically).

3.2 Monthly climate-growth relationships

The sensitivity of *P. pepei* RW to local climate between 1960-2015 is illustrated by bootstrapped correlations between monthly Pre, Tavg, Tmin, and Tmax in Fig. 3. *P. pepei* RW (standard chronology) positively correlates with Pre variability during the

wet season (Fig.3A). There are significant correlations between RW and prior (lag=1) December-March precipitation (r=0.37 for January). Correlations with prior-year December (r=0.20) weakened when controlling for Tavg, but current-year November Pre remains robust (r_p=0.27). Fig. A4A shows December-March (DJFM) precipitation significantly decreased over the 1960-2015 period at a rate of ~6 mm per decade at the same time there was an observed decline in *P. pepei* RW (Fig. 2A).

RW is negatively correlated to prior-year Tavg DJFM (r=-0.21 in March to r=-0.34 in February, $p<0.05$). However, after controlling for precipitation effects, partial correlations for Tavg revealed a positive, robust relationship ($p<0.05$) with RW current-year February to April (FMA) months (r_p= 0.25 in February to 0.37 in April). *P. pepei* RW also correlates positively with FMA Tmax (Fig. 2D), emphasizing the importance of late-wet season temperature variability near our site on current-year RW as well. Although there were no significant trends in FMA Tavg between 1960-2015 (Fig. A4 B), there was a significant decrease of Tmax FMA of nearly 0.1°C per decade (Fig. A4 D, p=0.05).

Unlike Tavg, partial correlations indicate RW correlations with prior-year Tmin (Fig. 3C) are significant independent of precipitation variability (i.e. the negative signal persists even when the covariance with precipitation is removed). Negative, significant correlations were found between *P. pepei* RW and prior November- March Tmin (NDJF; r=-0.28 in November to r=-0.35 in February). It is interesting to note an extreme cold period near Keara during the late 1950s (Tmin. Fig. A5 BC) corresponds with a growth suppression observed in *P. pepei* RW in Fig. 2A and C. Unlike the decrease observed in Tmax near Keara (FMA), NDJF Tmin significantly increased at a rate of 0.1°C per decade (p=0.02). In summary *Polylepis pepei* RW is limited by FMA Tmax (positive, current-year relationship) and NDJF Tmin (negative, lagged relationship) for distinct seasons.

Overall *Polylepis pepei* RW is larger under wetter and cooler conditions. However, climate trends since 1960 (Fig. A4) indicate this treeline is facing a warmer and drier November-March (Pre, Tmin) and a cooler wet-to-dry 'shoulder season' months between February- April (Tmax). As mentioned in Section 2.1, Tavg and Pre are negatively correlated during the wet season (~October-April, r=-0.27) in Keara and thus the robust negative correlations between RW temperature (Tmin, Tmax) emphasize the indirect effect of temperature on water availability and thus *P. pepei* tree-growth at treeline. Seasonal averages of DJFM precipitation, NDJF Tmin and FMA Tmax were selected for spatial correlation analyses for the greater tropical south American region.

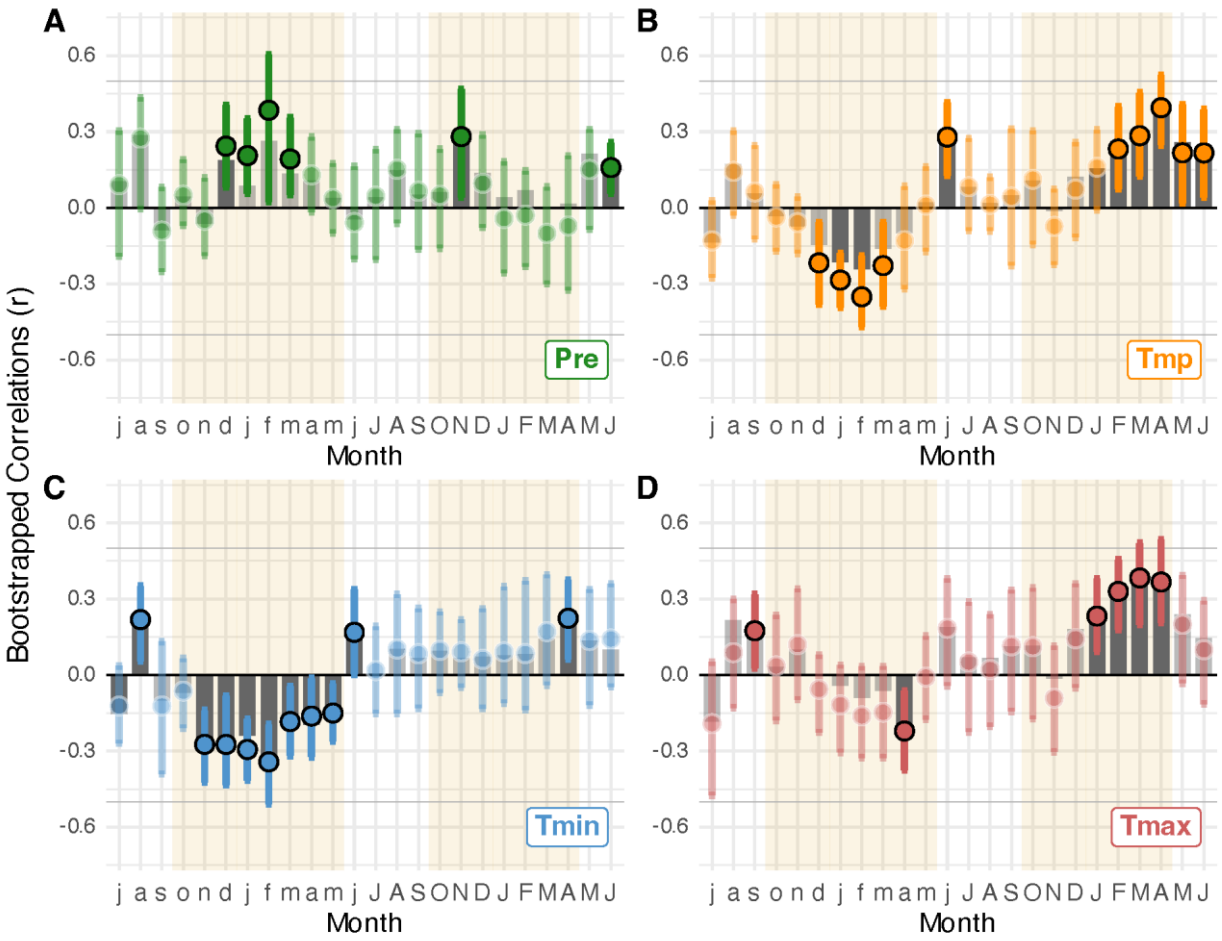

Figure 3: Bootstrapped correlations between *P. pepei* RW and monthly climate from 1960-2015. The x-axis represents months beginning in July of the prior-year (lag=1, lowercase letters) and extending to June of the current year (lag=0, uppercase letters). Tan shading indicates the extended wet period (~October- April) for this region of the MNP A: green color, precipitation from local station data. B-D: correlations with CRU temperature grid points Tavg(orange), Tmin (Blue), Tmax(red). The median Pearson correlation (*r*) is represented by colored circles plotted with upper and lower limits of confidence intervals. Partial correlations (r_p) are represented by grey bars. Solid circles and bars indicate significant correlations which are inferred from 95% confidence intervals from the random bootstrapping.

3.3. *Polylepis pepei* RW and tropical South American climate variability

Spatial correlations reveal the broader, regional extent of the climate signal recorded in the *P. pepei* RW at the Keara treeline. (Fig. 4). Binomial field tests indicated the spatial extent of significant correlations (black dots; $p<0.05$) exceeded what would be expected by chance ($p<0.001$ for all variables). *P. pepei* RW is positively correlated to prior-year DJFM precipitation (CHIRPS; 1981-2015) in most of tropical South America (Fig. 4A). The strongest precipitation signal is observed along the eastern flanks of the Peruvian Andes and the northern Amazon Basin in Brazil. RW is also positively correlated to FMA Tmax in the northern and southern portions of the tropical Andes-Amazon with the strongest values ($r > 0.50$) centralized locally

near the Bolivian Altiplano. Spatial correlations between *P. pepei* RW and prior-year NDJF Tmin (CRU 1960-2015) showed significant and negative correlations across most of tropical South America (Fig. 4C), especially near southeastern potions of Brazil. The RW-precipitation correlations also reflect the heterogeneity of precipitation data in mountain areas, whereas the temperature fields are more uniform.

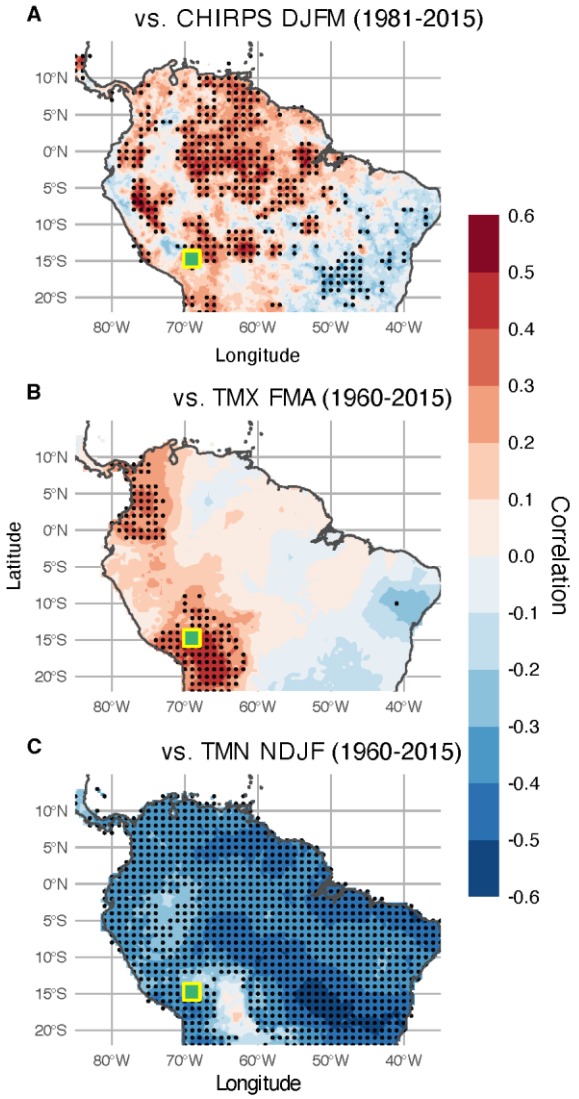

Figure 4. Spatial correlations between *P. pepei* RW and (A) CHIRPS DJFM precipitation (1981-2015, lag=1), (B) CRU NDJF Tmin (1960-2015, lag=1), and (C) CRU FMA Tmax (1960-2015, lag=0). Black dots represent the areas where there are significant correlations ($p<0.05$). Binomial field tests indicated there were more significant cells than expected by chance ($p=0.05$) for all variables (field test $p<0.001$).

3.4 Growth response of treeline *P. pepei* to extreme climate events

The impact of extreme DJF-ENSO events on climate and the residual RW chronology is shown in Figure 5. Table A1 lists the years of known moisture anomalies in tropical South America connected to El Niño (warmer SST) or La Niña (cooler SST) conditions in the Pacific Ocean. Regardless of the time span and spatial resolution, climate datasets show El Niño-DJF events were linked to drier and warmer conditions while extreme La Niña-DJF years were wetter and cooler (Fig. 5AB).

SEA results for El Niño-DJF years show there was a one-year delayed and negative RW response, i.e., one year after an event, *P. pepei* showed a decrease in radial growth ($\alpha = 0.1$). Although there was a non-significant growth increase in RW after a La Niña-DJF, there was a significant negative response three years after an extreme DJF-La Niña (Fig. 5B). It's interesting to note however, the largest growth ring observed in *P. pepei* formed during the 1950-1951 wet season and correspond to extreme La Niña events in DJF 1950 and 1951 (Fig.2C). The smallest (5^{th} percentile) growth ring in 1906-07 occurred after a major DJF-El Niño event in 1905. In summary, *P. pepei* RW at the Andes-Amazon treeline has a lagged significant response to extreme DJF-ENSO conditions.

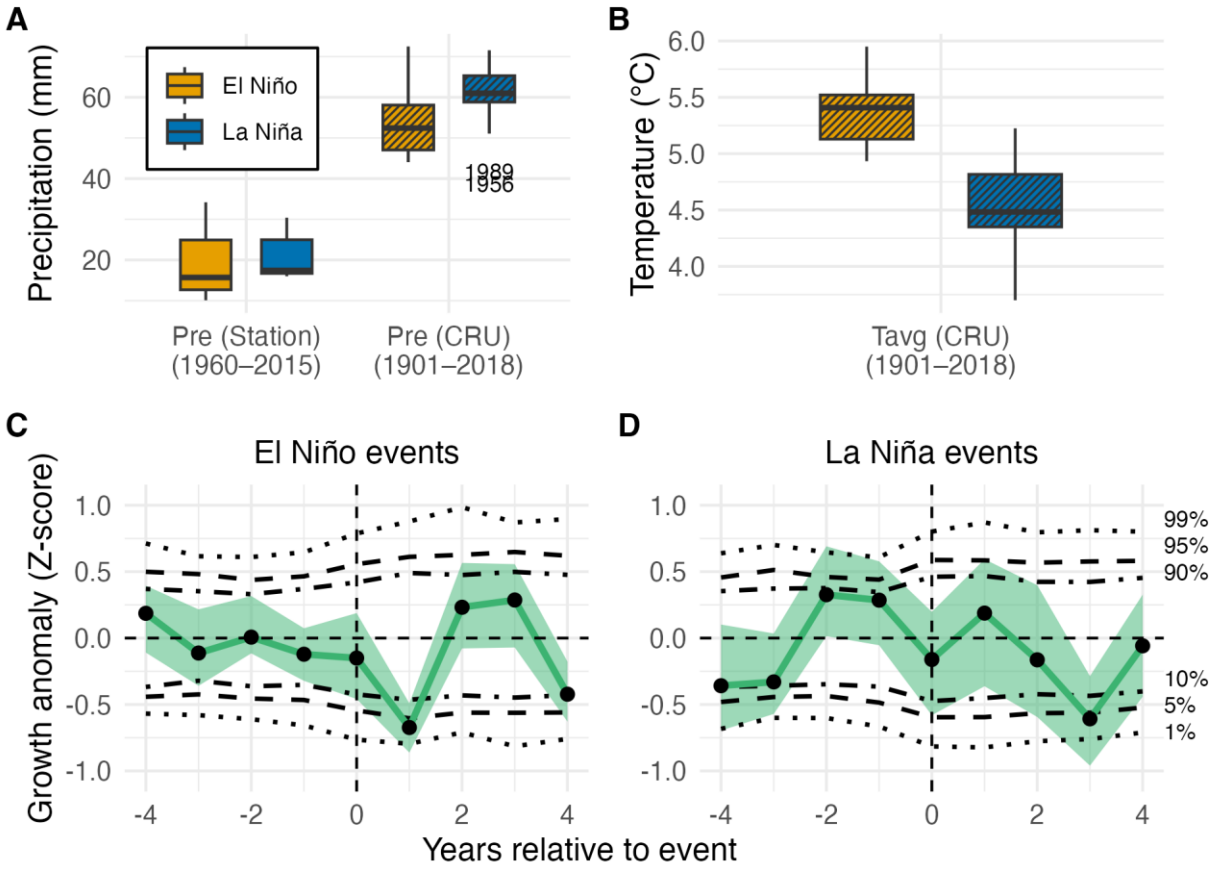

Figure 5: Boxplots showing annual (A) precipitation and (B) temperature for the 26 years of extreme DJF-ENSO events, using both station and CRU data. Outlier years in the CRU precipitation data are labeled in (A). Annual mean climate during El Nino-DJF is represented as orange colors, while La Niña is shown in blue (n = 13 years per event). Superposed epoch analysis of the residual RW response between 4 years before and 4 years after ENSO events (C, D). The uncertainty of the growth response is depicted as green shading. Horizontal black lines represent confidence intervals (two-tailed significance thresholds: 10-90%, 5-95% 1-99%) based on stationary bootstrapping.

4 Discussion

4.1. Radial growth decline and climate sensitivity of a tropical treeline site in Bolivia

Annual RW chronologies of *P. pepei* from a high Andean-Amazon forest in Bolivia have been presented and analyzed. This is the first tree-ring record for this species in Madidi National Park and the longest record of *P. pepei* RW chronology in South America (1850-2018). This record provides new information about tree growth and climate sensitivity in an understudied tropical treeline in South America (~3800-4400 m.a.s.l.). The potential human influence on RW for trees in Andes-Amazon forests should be considered when evaluating the growth patterns at tropical treelines in this region. For the *P. pepei* near Keara, the lower elevation open-canopy forest (3795-4100 m.a.s.l.) showed possible fire scars in the 1940s and clear forest fragmentation related to cattle ranching. This subpopulation is likely more threatened by human activities than the closed canopy site between 4000-4400 m.a.s.l. sampled in 2019 (Fig. 1CD). Despite the potential for local environmental effects on growth, correlations between *P. pepei* RW and local with climate are robust and may signify a response to regional shifts in hydroclimate patterns observed in tropical South America.

We found that *P. pepei* RW is limited by prior-year temperature and precipitation variability during the wet season, with larger RW in the subsequent growth year when it was wetter and colder (Figs. 3 and 4). This is consistent with previous studies showing *Polylepis* ring-width positively correlated with previous growing-season water availability in the Andes (Argollo et al. 2004, Morales et al. 2004, Christie et al. 2009, Soliz et al. 2009, Crispín-DelaCruz et al. 2022, Rodriguez-Caton. et a. 2021). Although the RW-precipitation correlations were robust, our results suggest that this *P. pepei* treeline is likely more affected by temperature-related moisture-stress changes (Fig. A4), as would be expected particularly at treeline (Fritts, 1976). A pronounced decline in radial growth since 1997 (Fig. 2A) was observed at the same time this region has endured warmer and drier austral summers (~November-March) in recent decades (Figs. A4, A5). The Keara treeline also revealed an imprint of extreme ENSO-related events in *P. pepei* growth rings.

Hot-drought conditions related to DJF-El Niño events had a significant negative impact on radial growth of *P. pepei* at our study site. Although La Niña SEA were-inconclusive, the lagged negative effect (*t*-3) may be related to the occurrence of El Niño events in years after La Niña. DJF anomalies were selected for analyses because it is the mature phase of the summer monsoon (70% of annual rainfall), but the use of annual (instead of seasonal) events may show larger impacts on RW.

Future advances of this treeline towards higher elevations (Fig. 1C) are unlikely due to local geomorphologic constraints (Macias-Fauria and Johnson, 2013) and thermal niches that are required for subalpine recruitment (Kessler et al., 2014; Körner and Hoch, 2023). As mentioned in the Introduction, *Polylepis pepei* in the tropical Andes is adapted to cold soil temperatures (3-5°C). Although the future spatial extent of the *P. pepei* forest under warming is uncertain, our study provides insight into

the limiting factors to radial growth at a tropical Andean treeline in Bolivia since 1960. In the following sections we discuss potential local environmental and climate variables that may contribute *P. pepei* tree-ring variability in Keara.

4.2. Changes in temperatures and humidity at the *P. pepei* treeline in Bolivia

Increases in minimum temperature (Tmin) may be reducing moisture availability in high-elevation Andean tropical sites. Hourly climate data recorded by data loggers at our *P. pepei* site (Fig. A3) showed that the period September 2021-May 2022 had significantly warmer Tmin and lower relative humidity (RH) in comparison to the period 2011-2014 ($p < 0.0001$). This decrease in RH alongside an increase in temperature suggests that the capacity of air to hold moisture has outpaced the actual moisture content, making the air drier despite higher temperatures. Although these results cover a short time-window, they provide in situ evidence of warming and drying trends observed in the climate data of this site (Fig. A4). DTR variability (i.e. difference between Tmax and Tmin) near Keara in Fig. A5 depicts a significant negative trend in this region since 1960, which means the rate of increase for minimum temperatures has surpassed that of maximum temperature. Even though warmer temperatures increase the capacity of the air to hold more water vapor (i.e., the Clausius-Clapeyron relation), if the moisture supply does not increase proportionally, humidity will decrease.

P. pepei had significant negative correlations with increasing minimum temperatures on the local and spatial scale (Figs. 3 and 4). Minimum temperatures influence convection, as rainfall in the Andes-Amazon ecotone largely occurs in the afternoon/night when radiative cooling drives cold air downslope and converges with rising warm moist air from the tropical lowlands (Garreaud, 1999; Junquas et al., 2018; Romatschke and Houze, 2010). Known as 'orographic precipitation', this process is key for rainfall distribution across elevations in the Andean foothills like our site (Arias et al., 2021; Chavez and Takahashi, 2017). In the region of the MNP, maximum precipitation occurred between 1000-1300 m.a.s.l., with a sharp decrease in moisture distribution towards higher elevations > 3000 m.a.s.l. (Chavez and Takahashi, 2017). If minimum temperatures increase, the radiative cooling effect is weaker, which may result in warm, moist air converging at lower elevations, below our treeline *P. pepei* site (Romatschke and Houze, 2010). The hourly meteorological data between September-May in 2011-14 and 2022-23 shows that RH peaks at 3:00 P.M. in Keara on average, suggesting afternoon cloud formation. It's interesting to note the declining RW trends observed in *P. pepei* (>3800 m.a.s.l.) diverge from the increasing RW trends observed in lower-elevation humid forests from MNP since the 1980s (*e.g. Juglans boliviana* ~1300 m.a.s.l., Oelkers et al. 2023). It is possible that the increase in Tmin since the late 20th century (Fig. A5) may have contributed to reduced orographic convection and moisture availability, thus potentially limiting the growth of *P. pepei*. Future research needs to be conducted on horizontal moisture transport in the Andes-Amazon and the diverging trends in growth between the lower Amazon and treeline forests.

Besides inhibiting moisture convergence and transport from lower elevations, warmer minimum temperatures could also affect the tree water-balance in Keara by increasing transpiration and respiration rates (Sierra et al., 2022). A global analysis of tropical tree longevity using tree-ring and other data found that tree mortality is increasing in all tropical biomes due to heat-

related water stress and increased evaporative demand at the leaf level (Locosselli et al., 2020). From an ecophysiological perspective, respiration rates increase with rising temperatures and without photosynthesis occurring at night. This in turn increases the amount of carbon (and water) released from the trees to the atmosphere.-Temperature and precipitation near the *P. pepei* site are inversely correlated during the extended wet season (October-April, $p<0.05$). If there is less cloud cover (and rainfall), there is higher solar irradiance and temperatures, which may limit the photosynthetic capacity of tropical trees at higher elevations (García-Núñez et al., 2004; Hoch and Körner, 2005; Jaramillo, 2015). The current-year positive relationship between RW and FMA Tmax (Fig.3C, Fig. 4.B), may also highlight the ecophysiological link between tree-ring size (i.e. xylogenesis) and cooler trends in Tmax at the end of the wet season between 1960-2015 (see discussion in Rodriguez-Caton et al. 2021). Although it is possible that the timing of the mechanisms controlling primary (photosynthesis) and secondary growth (wood formation) may not occur at the same time, the RW-climate correlations show there is less radial growth if is warmer and drier than when it is cooler and wetter (Figs. 3, A4). Further research must be conducted to determine the phenology and physiological response of *P. pepei* to micro-climate conditions such as a reduction in orographic precipitation at treeline or low soil-water availability.

4.3. Large-scale climate variability impacting tree growth in tropical Andean treelines

The recent decline in radial growth may be also influenced by broader scale hydroclimate changes. In the central Andes treeline, (>17°S; 4657-4800 m.a.s.l.). Negative RW trends in *P. tarapacana* were attributed to increasing drought conditions in southern Peru and northern Chile since the 1970s. *Morales* et al. (2023) developed a NDJ precipitation reconstruction from these trees and discovered that a drying trend since 1997 was unprecedented in the 389-yr reconstruction. Although 1997 was identified as a changepoint in the raw ring-width data of *P. pepei*, our site is in the Amazon basin, a much more humid environment than the *P. tarapacana* in *Morales* et al. (2023). Nonetheless the shared timing of growth decline in these high-Andes forests is interesting.

Increasing drought frequency in the tropical Andes and southern Amazon Basin (> ~15°S) has been linked to delayed wet season onset (Espinoza et al., 2016; Fu et al., 2013; Marengo et al., 2011). One possible explanation is an intensification of the atmospheric Hadley circulation, related to warming in the (northern) tropical Atlantic Ocean, which interrupts upward flows from the Amazon to the Andes during the dry-to-wet period (Beveridge et al., 2024; Espinoza et al., 2021, 2019; Yoon and Zeng, 2010). In particular, *Ronchail* et al. (2018) and *Espinoza* et al. (2019) found a significant increase in dry-day frequency between September-November in Bolivia and Peru which marks a delay in the timing of austral spring rainfall. Additionally, an observed weakening of upper-level easterlies winds from the Amazon to the Andes (Segura et al. 2022), may have contributed to reduced moisture transport potentially affecting tropical treelines like *P. pepei* in Keara.

In contrast to a drier start to the wet-season, a recent increase in precipitation at the end of the wet season < 2000 m.a.s.l. has been observed in lowland regions of the northern Amazon and Andes-Amazon (Arias et al., 2021; Espinoza et al., 2021, 2019;

Malhi et al., 2008; Zanin and Satyamurty, 2020). These studies argue that warming of the Atlantic Ocean, land-surface changes in the Amazon, and wind anomalies are the primary factors contributing to changes in specific humidity in tropical south America overall (particularly between March-May; see references in (Beveridge et al., 2024)). Within Bolivia, contrasting trends in precipitation and tree-growth have been observed between low and highland elevation forests. Tree-ring oxygen isotopes ($\delta^{18}O$ from *C. odorata* in the lowland Bolivian Amazon (10°5′S, 66°18′W; 106 m.a.s.l.) reflected an increase in November-March precipitation (and decrease in $\delta^{18}O$) between 1980-2010 (Baker et al., 2016; Cintra et al., 2025), while treeline *P. tarapacana* in the Bolivian Altiplano (22.3°S, 67.23°W; ~4600 m.a.s.l.) recorded a pronounced dry period for December-March precipitation between 1992-2012 (Rodriguez-Caton et al., 2024). Despite the fact that these hydroclimate trends are complex and spatially variable, having *in situ* high-resolution climate proxies at the Andes-Amazon treeline such as *P. pepei* may be useful in understanding long-term changes in orography.

Overall, growth variability at this *P. pepei* treeline in the Andes-Amazon here may be related to temperature-driven moisture trends observed at local and regional scales. This study herein has demonstrated the dendroclimatic potential of this species at a treeline from the most biodiverse region of the world (MNP; Muller, 2017) and provided insight into the growth response of a tropical forest in South America under a warming environment.

5 Conclusions

We reported a significant decline in radial growth in a tropical *P. pepei* treeline in Keara, Bolivia, at the edges of the Andes-Amazon high-elevation forests. Here, grow decreases with warmer and drier conditions in the prior-year wet season, and there is an adverse influence of temperatures, in particular Tmin, on growth. Higher Tmin weakens the nighttime convection that brings moisture from lower elevations to this site, and in general, warmer conditions increase evaporative demands and cause water stresses. We also found a tendency of narrower growth rings in the year following El Niño events, while the role of La Niña events was inconclusive. This asymmetric influence of ENSO on tree growth warrants further investigations. Moving forward, since we found *P. pepei* to develop annual rings that are climate sensitive, expanding the *P. pepei* network in Keara would enable reconstructions of precipitation and temperature of the southwestern Amazon-Andes ecotone. This would be the first of its kind for northern Bolivia, extending the limited station records to the mid-1800s. Our results provide new insights into the response of a tropical treeline in an era of global warming, increasing climate extremes, and human activities, and support future dendrochronological research of *P. pepei* in South America. We recommend pursuing research that focus on quantifying leaf respiration and temperature response to better understand the ecophysiology of this tropical treeline species in Bolivia.

Author contribution

Co-authors LAH, DRC, MRC, MEF, RO, ET, AF collected tree samples in Keara. CM and AF organized field campaigns and provided essential information regarding Madid National Park. RDD and LAH assisted in initial experimental design and editing. Tree-ring dating, measuring, and analyses was conducted by corresponding other RO. HTTN, aided in correlation analyses and concept. APS assisted in wood anatomical methods. Editorial review provided by all co-authors. Site images for Fig. 1 were taken by RO.

Competing interests

The authors declare that they have no conflict of interest

Acknowledgements

This work was made possible by the following funding sources from the U.S. National Science Foundation: AGS-1702789, AGS-1903687, AGS-2303524, and OISE-1743738. We acknowledge the NSF AGS-1903690 grant at UC Irvine KCCAMS facility for seven radiocarbon measurements. E.T. received funding from the Comunidad de Madrid program Atracción Talento "César Nombela" grant number 2023-T1/ECO-29118. This work is dedicated to Renaud, his family and the community of Keara for their hospitality, knowledge, and assistance in the field. Special thanks the Nacional Herbario in La Paz, including Alfredo Fuentes and Freddy "Zen" Ruiz, for their guidance during the 2012 and 2019, 2023 Bolivian field campaigns.

Data Availability

The Polylepis pepei RW chronology from Keara will be made publicly available on the NOAA International Tree-ring Database.

References

Argollo, J., Soliz, C., Villalba, R., 2004. Potencialidad dendrocronológica de Polylepis tarapacana en los Andes Centrales de Bolivia. Ecol. En Boliv. 39, 5–24.

Büntgen, U., Wacker, L., Galván, J.D., Arnold, S., Arseneault, D., Baillie, M., Beer, J., Bernabei, M., Bleicher, N., Boswijk, G., Bräuning, A., Carrer, M., Ljungqvist, F.C., Cherubini, P., Christl, M., Christie, D.A., Clark, P.W., Cook, E.R., D'Arrigo, R., Davi, N., Eggertsson, Ó., Esper, J., Fowler, A.M., Gedalof, Z., Gennaretti, F., Grießinger, J., Grissino-Mayer, H., Grudd, H., Gunnarson, B.E., Hantemirov, R., Herzig, F., Hessl, A., Heussner, K.-U., Jull, A.J.T., Kukarskih, V., Kirdyanov, A., Kolář, T., Krusic, P.J., Kyncl, T., Lara, A., LeQuesne, C., Linderholm, H.W., Loader, N.J., Luckman, B., Miyake, F., Myglan, V.S., Nicolussi, K., Oppenheimer, C., Palmer, J., Panyushkina, I., Pederson, N., Rybníček, M., Schweingruber, F.H., Seim, A., Sigl, M., Churakova (Sidorova), O., Speer, J.H., Synal, H.-A., Tegel, W., Treydte, K., Villalba, R., Wiles, G., Wilson, R., Winship, L.J., Wunder, J., Yang, B., Young, G.H.F., 2018. Tree rings reveal globally coherent signature of cosmogenic radiocarbon events in 774 and 993 CE. Nat. Commun. 9, 3605. https://doi.org/10.1038/s41467-018-06036-0

Crispín-DelaCruz, D.B., Morales, Mariano.S., Andreu-Hayles, Laia., Christie, Duncan.A., Guerra, A., Requena-Rojas, Edilson.J., 2022. High ENSO sensitivity in tree rings from a northern population of Polylepis tarapacana in the Peruvian Andes. Dendrochronologia 71, 125902. https://doi.org/10.1016/j.dendro.2021.125902

D'Arrigo, R., Jacoby, G., Free, M., Robock, A., 1999. Northern Hemisphere Temperature Variability for the Past Three Centuries: Tree-Ring and Model Estimates. Clim. Change 42, 663–675. https://doi.org/10.1023/A:1005471918574

Farfan-Rios, W., Feeley, K.J., Myers, J.A., Tello, S., Sallo-Bravo, J., Malhi, Y., Phillips, O.L., Baker, T.R., Nina-Quispe, A., Garcia-Cabrera, K., 2025. Amazonian and Andean tree communities are not tracking current climate warming. Proc. Natl. Acad. Sci. 122, e2425619122.

MacDonald, G. m, Kremenetski, K. v, Beilman, D. w, 2007. Climate change and the northern Russian treeline zone. Philos. Trans. R. Soc. B Biol. Sci. 363, 2283–2299. https://doi.org/10.1098/rstb.2007.2200

Politis, D.N., Romano, J.P., 1994. The Stationary Bootstrap. J. Am. Stat. Assoc. 89, 1303–1313. https://doi.org/10.1080/01621459.1994.10476870

Rodriguez-Caton, M., Andreu-Hayles, L., Daux, V., Vuille, M., Varuolo-Clarke, A.M., Oelkers, R., Christie, D.A., D'Arrigo, R., Morales, M.S., Palat Rao, M., Srur, A.M., Vimeux, F., Villalba, R., 2022. Hydroclimate and ENSO Variability Recorded by Oxygen Isotopes From Tree Rings in the South American Altiplano. Geophys. Res. Lett. 49. https://doi.org/10.1029/2021GL095883

Rodriguez-Caton, M., Andreu-Hayles, L., Morales, M.S., Daux, V., Christie, D.A., Coopman, R.E., Alvarez, C., Rao, M.P., Aliste, D., Flores, F., Villalba, R., 2021. Different climate sensitivity for radial growth, but uniform for tree-ring stable isotopes along an aridity gradient in Polylepis tarapacana, the world's highest elevation tree species. Tree Physiol. 41, 1353–1371. https://doi.org/10.1093/treephys/tpab021

Rodriguez-Caton, M., Morales, M.S., Rao, M.P., Nixon, T., Vuille, M., Rivera, J.A., Oelkers, R., Christie, D.A., Varuolo-Clarke, A.M., Ferrero, M.E., Magney, T., Daux, V., Villalba, R., Andreu-Hayles, L., 2024. A 300-year tree-ring δ18O-based precipitation reconstruction for the South American Altiplano highlights decadal hydroclimate teleconnections. Commun. Earth Environ. 5, 1–13. https://doi.org/10.1038/s43247-024-01385-9

Akaike, H., 1974. A new look at the statistical model identification. IEEE Trans. Autom. Control 19, 716–723.

Álvarez, C., Veblen, T.T., Christie, D.A., González-Reyes, Á., 2015. Relationships between climate variability and radial growth of *Nothofagus pumilio* near altitudinal treeline in the Andes of northern Patagonia, Chile. For. Ecol. Manag. 342, 112–121. https://doi.org/10.1016/j.foreco.2015.01.018

Andreu-Hayles, L., Tejedor, E., D'Arrigo, R., Locosselli, G.M., Rodríguez-Catón, M., Daux, V., Oelkers, R., Pacheco-Solana, A., Paredes-Villanueva, K., Rodríguez-Morata, C., 2023. Dendrochronological advances in the tropical and subtropical Americas: Research priorities and future directions. Dendrochronologia 81, 126124. https://doi.org/10.1016/j.dendro.2023.126124

Arias, P.A., Garreaud, R., Poveda, G., Espinoza, J.C., Molina-Carpio, J., Masiokas, M., Viale, M., Scaff, L., van Oevelen, P.J., 2021. Hydroclimate of the Andes Part II: Hydroclimate Variability and Sub-Continental Patterns. Front. Earth Sci. 8. https://doi.org/10.3389/feart.2020.505467

Batllori, E., Gutiérrez, E., 2008. Regional tree line dynamics in response to global change in the Pyrenees. J. Ecol. 96, 1275–1288. https://doi.org/10.1111/j.1365-2745.2008.01429.x

Beveridge, C.F., Espinoza, J.-C., Athayde, S., Correa, S.B., Couto, T.B.A., Heilpern, S.A., Jenkins, C.N., Piland, N.C., Utsunomiya, R., Wongchuig, S., Anderson, E.P., 2024. The Andes–Amazon–Atlantic pathway: A foundational hydroclimate system for social–ecological system sustainability. Proc. Natl. Acad. Sci. 121, e2306229121. https://doi.org/10.1073/pnas.2306229121

Buras, A., 2017. A comment on the expressed population signal. Dendrochronologia 44, 130–132. https://doi.org/10.1016/j.dendro.2017.03.005

Camarero, J.J., Mendivelso, H.A., Sánchez-Salguero, R., 2020. How Past and Future Climate and Drought Drive Radial-Growth Variability of Three Tree Species in a Bolivian Tropical Dry Forest, in: Pompa-García, M., Camarero, J.J. (Eds.), Latin American Dendroecology: Combining Tree-Ring Sciences and Ecology in a Megadiverse Territory. Springer International Publishing, Cham, pp. 141–167. https://doi.org/10.1007/978-3-030-36930-9_7

Chavez, S.P., Takahashi, K., 2017. Orographic rainfall hot spots in the Andes-Amazon transition according to the TRMM precipitation radar and in situ data. J. Geophys. Res. Atmospheres 122, 5870–5882. https://doi.org/10.1002/2016JD026282

Cook, E.R., Briffa, K.R., Shiyatov, S., Mazepa, V., 1990. Tree-ring standardization and growth-trend estimation 104–123.

Cook, E.R., Peters, K., 1981. The Smoothing Spline: A New Approach to Standardizing Forest Interior Tree-Ring Width Series for Dendroclimatic Studies.

Cuesta, F., Tovar, C., Llambí, L.D., Gosling, W.D., Halloy, S., Carilla, J., Muriel, P., Meneses, R.I., Beck, S., Ulloa Ulloa, C., Yager, K., Aguirre, N., Viñas, P., Jácome, J., Suárez-Duque, D., Buytaert, W., Pauli, H., 2020. Thermal niche traits of high alpine plant species and communities across the tropical Andes and their vulnerability to global warming. J. Biogeogr. 47, 408–420. https://doi.org/10.1111/jbi.13759

Cuyckens, G.A.E., Christie, D.A., Domic, A.I., Malizia, L.R., Renison, D., 2016. Climate change and the distribution and conservation of the world's highest elevation woodlands in the South American Altiplano. Glob. Planet. Change 137, 79–87. https://doi.org/10.1016/j.gloplacha.2015.12.010

Cybis Elektronik, 2010. CDendro and CooRecorder [WWW Document]. URL http://www.cybis.se/forfun/dendro/index.htm

D'Arrigo, R., Wilson, R., Liepert, B., Cherubini, P., 2008. On the 'Divergence Problem' in Northern Forests: A review of the tree-ring evidence and possible causes. Glob. Planet. Change 60, 289–305. https://doi.org/10.1016/j.gloplacha.2007.03.004

D'Arrigo, R.D., Kaufmann, R.K., Davi, N., Jacoby, G.C., Laskowski, C., Myneni, R.B., Cherubini, P., 2004. Thresholds for warming-induced growth decline at elevational tree line in the Yukon Territory, Canada. Glob. Biogeochem. Cycles 18. https://doi.org/10.1029/2004GB002249

Devi, N.M., Kukarskih, V.V., Galimova, A.A., Mazepa, V.S., Grigoriev, A.A., 2020. Climate change evidence in tree growth and stand productivity at the upper treeline ecotone in the Polar Ural Mountains. For. Ecosyst. 7, 7. https://doi.org/10.1186/s40663-020-0216-9

Duque, A., Peña, M.A., Cuesta, F., González-Caro, S., Kennedy, P., Phillips, O.L., Calderón-Loor, M., Blundo, C., Carilla, J., Cayola, L., Farfán-Ríos, W., Fuentes, A., Grau, R., Homeier, J., Loza-Rivera, M.I., Malhi, Y., Malizia, A., Malizia, L., Martínez-Villa, J.A., Myers, J.A., Osinaga-Acosta, O., Peralvo, M., Pinto, E., Saatchi, S., Silman, M., Tello, J.S., Terán-Valdez, A., Feeley, K.J., 2021. Mature Andean forests as globally important carbon sinks and future carbon refuges. Nat. Commun. 12, 2138. https://doi.org/10.1038/s41467-021-22459-8

Enfield, D.B., Mestas-Nuñez, A.M., Mayer, D.A., Cid-Serrano, L., 1999. How ubiquitous is the dipole relationship in tropical Atlantic sea surface temperatures? J. Geophys. Res. Oceans 104, 7841–7848. https://doi.org/10.1029/1998JC900109

Espinoza, J.-C., Arias, P.A., Moron, V., Junquas, C., Segura, H., Sierra-Pérez, J.P., Wongchuig, S., Condom, T., 2021. Recent Changes in the Atmospheric Circulation Patterns during the Dry-to-Wet Transition Season in South Tropical South America (1979–2020): Impacts on Precipitation and Fire Season. J. Clim. 34, 9025–9042. https://doi.org/10.1175/JCLI-D-21-0303.1

Espinoza, J.C., Ronchail, J., Marengo, J.A., Segura, H., 2019. Contrasting North–South changes in Amazon wet-day and dry-day frequency and related atmospheric features (1981–2017). Clim. Dyn. 52, 5413–5430. https://doi.org/10.1007/s00382-018-4462-2

Espinoza, J.C., Segura, H., Ronchail, J., Drapeau, G., Gutierrez-Cori, O., 2016. Evolution of wet-day and dry-day frequency in the western Amazon basin: Relationship with atmospheric circulation and impacts on vegetation. Water Resour. Res. 52, 8546–8560. https://doi.org/10.1002/2016WR019305

Espinoza, T.E.B., Kessler, M., 2022. A monograph of the genus Polylepis (Rosaceae). PhytoKeys 203, 1–274. https://doi.org/10.3897/phytokeys.203.83529

Feeley, K.J., Rehm, E.M., Machovina, B., 2012. perspective: The responses of tropical forest species to global climate change: acclimate, adapt, migrate, or go extinct? Front. Biogeogr. 4. https://doi.org/10.21425/F5FBG12621

Feeley, K.J., Silman, M.R., Bush, M.B., Farfan, W., Cabrera, K.G., Malhi, Y., Meir, P., Revilla, N.S., Quisiyupanqui, M.N.R., Saatchi, S., 2011. Upslope migration of Andean trees. J. Biogeogr. 38, 783–791. https://doi.org/10.1111/j.1365-2699.2010.02444.x

Ferrero, M.E., Villalba, R., De Membiela, M., Ripalta, A., Delgado, S., Paolini, L., 2013. Tree-growth responses across environmental gradients in subtropical Argentinean forests. Plant Ecol. 214, 1321–1334. https://doi.org/10.1007/s11258-013-0254-2

Finer, M., Mamani, N., 2023. Amazon Deforestation & Fire Hotspots 2022. MAAP 187, 2017–21.

Flynn, H., Camarero, J.J., Sanmiguel-Vallelado, A., Rojas Heredia, F., Domínguez Aguilar, P., Revuelto, J., López-Moreno, J.I., 2025. A shift in circadian stem increment patterns in a Pyrenean alpine treeline precedes spring growth after snow melting. Biogeosciences 22, 1135–1147. https://doi.org/10.5194/bg-22-1135-2025

Frank, D., Esper, J., Cook, E., 2006. On variance adjustments in tree-ring chronology development. Tree Rings Archaeol. Climatol. Ecol. TRACE 4, 56–66.

Fritts, H.C., 1976. Tree rings and Climate. Academic Press, London.

Fu, R., Yin, L., Li, W., Arias, P.A., Dickinson, R.E., Huang, L., Chakraborty, S., Fernandes, K., Liebmann, B., Fisher, R., Myneni, R.B., 2013. Increased dry-season length over southern Amazonia in recent decades and its implication for future climate projection. Proc. Natl. Acad. Sci. 110, 18110–18115. https://doi.org/10.1073/pnas.1302584110

Fuentes, A., 2005. Una introducción a la vegetación de la región de Madidi 32.

Funk, C., Peterson, P., Landsfeld, M., Pedreros, D., Verdin, J., Shukla, S., Husak, G., Rowland, J., Harrison, L., Hoell, A., 2015. The climate hazards infrared precipitation with stations—a new environmental record for monitoring extremes. Sci. Data 2, 1–21.

García-Núñez, C., Rada, F., Boero, C., González, J., Gallardo, M., Azócar, A., Liberman-Cruz, M., Hilal, M., Prado, F., 2004. Leaf Gas Exchange and Water Relations in Polylepis tarapacana at Extreme Altitudes in the Bolivian Andes. Photosynthetica 42, 133–138. https://doi.org/10.1023/B:PHOT.0000040581.94641.ed

Garreaud, R., 1999. Multiscale Analysis of the Summertime Precipitation over the Central Andes.

Garreaud, R.D., 2009. The Andes climate and weather. Adv. Geosci. 22, 3–11. https://doi.org/10.5194/adgeo-22-3-2009

Good, P., Lowe, J.A., Collins, M., Moufouma-Okia, W., 2008. An objective tropical Atlantic sea surface temperature gradient index for studies of south Amazon dry-season climate variability and change. Philos. Trans. R. Soc. B Biol. Sci. 363, 1761–1766. https://doi.org/10.1098/rstb.2007.0024

Groenendijk, P., Babst, F., Trouet, V., Fan, Z.-X., Granato-Souza, D., Locosselli, G.M., Mokria, M., Panthi, S., Pumijumnong, N., Abiyu, A., Acuña-Soto, R., Adenesky-Filho, E., Alfaro-Sánchez, R., Anholetto Junior, C.R., Aragão, J.R.V., Assis-Pereira, G., Astudillo-Sánchez, C.C., Carolina Barbosa, A., Barreto, N. de O., Battipaglia, G., Beeckman, H., Botosso, P.C., Bourland, N., Bräuning, A., Brienen, R., Brookhouse, M., Buajan, S., Buckley, B.M., Camarero, J.J., Carrillo-Parra, A., Ceccantini, G., Centeno-Erguera, L.R., Cerano-Paredes, J., Cervantes-Martínez, R., Chanthorn, W., Chen, Y.-J., Cintra, B.B.L., Cornejo-Oviedo, E.H., Cortés-Cortés, O., Costa, C.M., Couralet, C., Crispin-

DelaCruz, D.B., D'Arrigo, R., David, D.A., De Ridder, M., Del Valle, J.I., Díaz-Carrillo, O.A., Dobner Jr, M., Doucet, J.-L., Dünisch, O., Enquist, B.J., Esemann-Quadros, K., Esquivel-Arriaga, G., Fayolle, A., Fenilli, T.A.B., Ferrero, M.E., Fichtler, E., Finnegan, P.M., Fontana, C., Francisco, K.S., Fu, P.-L., Galvão, F., Gebrekirstos, A., Giraldo, J.A., Gloor, E., Godoy-Veiga, M., Guerra, A., Haneca, K., Harley, G.L., Heinrich, I., Helle, G., Hernández-Díaz, J.C., Hornink, B., Hubau, W., Inga, J.G., Islam, M., Jiang, Y., Kaib, M., Hassan Khamisi, Z., Koprowski, M., Layme, E., Leffler, A.J., Ligot, G., Lisi, C.S., Loader, N.J., Lobo, F. de A., Longhi-Santos, T., Lopez, L., López-Hernández, M.I., Lousada, J.L.P.C., Manzanedo, R.D., Marcon, A.K., Maxwell, J.T., Mendivelso, H.A., Mendoza-Villa, O.N., Menezes, Í.R.N., Montóia, V.R., Moors, E., Moreno, M., Muñiz-Castro, M.A., Nabais, C., Nathalang, A., Ngoma, J., Nogueira Jr., F. de C., Oliveira, J.M., Olmedo, G.M., Ortega-Rodriguez, D.R., Ortíz, C.E.R., Pagotto, M.A., Paredes-Villanueva, K., Pérez-De-Lis, G., Ponce Calderón, L.P., Portal-Cahuana, L.A., Pucha-Cofrep, D.A., Quadri, P., Rahman, M., Ramírez, J.A., Requena-Rojas, E.J., Reyes-Flores, J., Ribeiro, A. de S., Robertson, I., Roig, F.A., Roquette, J.G., Rubio-Camacho, E.A., Sánchez-Salguero, R., Sass-Klaassen, U., Schöngart, J., Scipioni, M.C., Sheppard, P.R., Silva, L.C.R., Slotta, F., Soria-Díaz, L., Sousa, L.K.V.S., Speer, J.H., Therrell, M.D., Ticse-Otarola, G., Tomazello-Filho, M., Torbenson, M.C.A., Tor-Ngern, P., Touchan, R., Van Den Bulcke, J., Vázquez-Selem, L., Velázquez-Pérez, A.H., Venegas-González, A., Villalba, R., Villanueva-Diaz, J., Vlam, M., Vourlitis, G., Wehenkel, C., Wils, T., Zavaleta, E.S., Zewdu, E.A., Zhang, Y.-J., Zhou, Z.-K., Zuidema, P.A., 2025. The importance of tropical tree-ring chronologies for global change research. Quat. Sci. Rev. 355, 109233. https://doi.org/10.1016/j.quascirev.2025.109233

Harris, I., Osborn, T.J., Jones, P., Lister, D., 2020. Version 4 of the CRU TS monthly high-resolution gridded multivariate climate dataset. Sci. Data 7, 109. https://doi.org/10.1038/s41597-020-0453-3

Haurwitz, M.W., Brier, G.W., 1981. A critique of the superposed epoch analysis method: its application to solar–weather relations. Mon. Weather Rev. 109, 2074–2079.

Hertel, D., Wesche, K., 2008. Tropical moist Polylepis stands at the treeline in East Bolivia: the effect of elevation on stand microclimate, above- and below-ground structure, and regeneration. Trees 22, 303–315. https://doi.org/10.1007/s00468-007-0185-4

Hoch, G., Körner, C., 2005. Growth, Demography and Carbon Relations of Polylepis Trees at the World's Highest Treeline. Funct. Ecol. 19, 941–951.

Hock, R., Rasul, G., Adler, C., Caceres, B., Gruber, S., Hirabayashi, Y., Jackson, M., Kääb, A., Kang, S., Kutuzov, S., Milner, A., Molau, U., Morin, S., Orlove, B., Steltzer, H., Allen, S., Arenson, L., Baneerjee, S., Barr, I., Bórquez, R., Brown, L., Cao, B., Carey, M., Cogley, G., Fischlin, A., A de Sherbinin, Eckert, N., Geertsema, M., Hagenstad, M., Honsberg, M., Hood, E., Huss, M., E Jimenez Zamora, Kotlarski, S., Lefeuvre, P., J Ignacio López Moreno, Lundquist, J., Mcdowell, G., Mills, S., Mou, C., Nepal, S., Noetzli, J., Palazzi, E., Pepin, N., Rixen, C., Shahgedanova, M., S McKenzie Skiles, Vincent, C., Viviroli, D., Gesa, A.W., P Yangjee Sherpa, Weyer, N., Wouters, B., Yasunari, T., You, Q., Zhang, Y., 2019. High Mountain Areas. STATI UNITI D'AMERICA.

Hoffmann, D., Weggenmann, D., 2013. Climate Change Induced Glacier Retreat and Risk Management: Glacial Lake Outburst Floods (GLOFs) in the Apolobamba Mountain Range, Bolivia, in: Leal Filho, W. (Ed.), Climate Change and Disaster Risk Management, Climate Change Management. Springer, Berlin, Heidelberg, pp. 71–87. https://doi.org/10.1007/978-3-642-31110-9_5

Hua, Q., Turnbull, J.C., Santos, G.M., Rakowski, A.Z., Ancapichún, S., Pol-Holz, R.D., Hammer, S., Lehman, S.J., Levin, I., Miller, J.B., Palmer, J.G., Turney, C.S.M., 2022. ATMOSPHERIC RADIOCARBON FOR THE PERIOD 1950–2019. Radiocarbon 64, 723–745. https://doi.org/10.1017/RDC.2021.95

Jacoby, G.C., D'Arrigo, R.D., 1995. Tree ring width and density evidence of climatic and potential forest change in Alaska. Glob. Biogeochem. Cycles 9, 227–234. https://doi.org/10.1029/95GB00321

Jaramillo, A.D., 2015. Fotosíntesis en los Bosques a Mayor Elevación en el Planeta: Polylepis tarapacana en un Gradiente de Elevación en los Andes de Arica y Parinacota, Chile.

Jomelli, V., Pavlova, I., Guin, O., Soliz-Gamboa, C., Contreras, A., Toivonen, J.M., Zetterberg, P., 2012. Analysis of the Dendroclimatic Potential of Polylepis pepei, P. subsericans and P. rugulosa In the Tropical Andes (Peru-Bolivia). Tree-Ring Res. 68, 91–103. https://doi.org/10.3959/2011-10.1

Junquas, C., Takahashi, K., Condom, T., Espinoza, J.-C., Chavez, S., Sicart, J.-E., Lebel, T., 2018. Understanding the influence of orography on the precipitation diurnal cycle and the associated atmospheric processes in the central Andes. Clim. Dyn. 50, 3995–4017. https://doi.org/10.1007/s00382-017-3858-8

Kessler, M., Toivonen, J.M., Sylvester, S.P., Kluge, J., Hertel, D., 2014. Elevational patterns of Polylepis tree height (Rosaceae) in the high Andes of Peru: role of human impact and climatic conditions. Front. Plant Sci. 5. https://doi.org/10.3389/fpls.2014.00194

Kolmogorov, A., 1933. Sulla determinazione empirica di una legge didistribuzione. Giorn Dellinst Ital Degli Att 4, 89–91.

Körner, C., 2012. Definitions and conventions, in: Körner, C. (Ed.), Alpine Treelines: Functional Ecology of the Global High Elevation Tree Limits. Springer, Basel, pp. 11–19. https://doi.org/10.1007/978-3-0348-0396-0_2

Körner, C., Hoch, G., 2023. Not every high-latitude or high-elevation forest edge is a treeline. J. Biogeogr. 50, 838–845. https://doi.org/10.1111/jbi.14593

Locosselli, G.M., Brienen, R.J.W., Leite, M. de S., Gloor, M., Krottenthaler, S., Oliveira, A.A. de, Barichivich, J., Anhuf, D., Ceccantini, G., Schöngart, J., Buckeridge, M., 2020. Global tree-ring analysis reveals rapid decrease in tropical tree longevity with temperature. Proc. Natl. Acad. Sci. 117, 33358–33364. https://doi.org/10.1073/pnas.2003873117

López, V.L., Huertas Herrera, A., Rosas, Y.M., Cellini, J.M., 2022. Optimal environmental drivers of high-mountains forest: *Polylepis tarapacana* cover evaluation in their southernmost distribution range of the Andes. Trees For. People 9, 100321. https://doi.org/10.1016/j.tfp.2022.100321

Macek, P., Macková, J., de Bello, F., 2009. Morphological and ecophysiological traits shaping altitudinal distribution of three Polylepis treeline species in the dry tropical Andes. Acta Oecologica 35, 778–785. https://doi.org/10.1016/j.actao.2009.08.013

Macía, M.J., 2008. Woody plants diversity, floristic composition and land use history in the Amazonian rain forests of Madidi National Park, Bolivia. Biodivers. Conserv. 17, 2671–2690. https://doi.org/10.1007/s10531-008-9348-x

Malhi, Y., Roberts, J.T., Betts, R.A., Killeen, T.J., Li, W., Nobre, C.A., 2008. Climate Change, Deforestation, and the Fate of the Amazon. Science 319, 169–172.

Malizia, A., Blundo, C., Carilla, J., Acosta, O.O., Cuesta, F., Duque, A., Aguirre, N., Aguirre, Z., Ataroff, M., Baez, S., Calderón-Loor, M., Cayola, L., Cayuela, L., Ceballos, S., Cedillo, H., Ríos, W.F., Feeley, K.J., Fuentes, A.F., Álvarez, L.E.G., Grau, R., Homeier, J., Jadan, O., Llambi, L.D., Rivera, M.I.L., Macía, M.J., Malhi, Y., Malizia, L., Peralvo, M., Pinto, E., Tello, S., Silman, M., Young, K.R., 2020. Elevation and latitude drives structure and tree species composition in Andean forests: Results from a large-scale plot network. PLOS ONE 15, e0231553. https://doi.org/10.1371/journal.pone.0231553

Marengo, J.A., Tomasella, J., Alves, L.M., Soares, W.R., Rodriguez, D.A., 2011. The drought of 2010 in the context of historical droughts in the Amazon region. Geophys. Res. Lett. 38. https://doi.org/10.1029/2011GL047436

Meko, D.M., Touchan, R., Anchukaitis, K.J., 2011. Seascorr: A MATLAB program for identifying the seasonal climate signal in an annual tree-ring time series. Comput. Geosci. 37, 1234–1241. https://doi.org/10.1016/j.cageo.2011.01.013

Melvin, T., 2004. Historical growth rates and changing climatic sensitivity of boreal conifers.

Montaño-Centellas, F., Fuentes, A.F., Cayola, L., Macía, M.J., Arellano, G., Loza, M.I., Nieto-Ariza, B., Tello, J.S., 2024. Elevational range sizes of woody plants increase with climate variability in the Tropical Andes. J. Biogeogr. 51, 814–826. https://doi.org/10.1111/jbi.14783

Morales, M.S., Crispín-DelaCruz, D.B., Álvarez, C., Christie, D.A., Ferrero, M.E., Andreu-Hayles, L., Villalba, R., Guerra, A., Ticse-Otarola, G., Rodríguez-Ramírez, E.C., LLoccla-Martínez, R., Sanchez-Ferrer, J., Requena-Rojas, E.J., 2023. Drought increase since the mid-20th century in the northern South American Altiplano revealed by a 389-year precipitation record. Clim. Past 19, 457–476. https://doi.org/10.5194/cp-19-457-2023

Morales, M.S., Villalba, R., Grau, H.R., Paolini, L., 2004. Rainfall-Controlled Tree Growth in High-Elevation Subtropical Treelines. Ecology 85, 3080–3089. https://doi.org/10.1890/04-0139

Muller, M.R., 2017. Protected areas and their relationship with food security in a context of climate change: an overview from Bolivia, Brazil and Peru. Prot. AREAS.

Navarro, G., Arrázola, S., Balderrama, J.A., Ferreira, W., De la Barra, N., Antezana, C., Gómez, I., Mercado, M., 2010. Diagnóstico del estado de conservación y caracterización de los bosques de Polylepis en Bolivia y su avifauna Conservation state analysis and characterization of the Bolivian Polylepis forests and their avifauna. Rev. Boliv. Ecol. Conserv. Ambient. 28, 1–35.

Oelkers, R.C., Andreu-Hayles, L., D'Arrigo, R., Pacheco-Solana, A., Rodriguez-Caton, M., Fuentes, A., Santos, G.M., Tejedor, E., Ferrero, M.E., Maldonado, C., 2023. Recent growth increase in endemic Juglans boliviana from the tropical Andes. Dendrochronologia 79, 126090. https://doi.org/10.1016/j.dendro.2023.126090

Paegle, J.N., Mo, K.C., 2002. Linkages between Summer Rainfall Variability over South America and Sea Surface Temperature Anomalies.

Paulsen, J., Weber ,U. M., and Körner, Ch., 2000. Tree Growth near Treeline: Abrupt or Gradual Reduction with Altitude? Arct. Antarct. Alp. Res. 32, 14–20. https://doi.org/10.1080/15230430.2000.12003334

Pettitt, A.N., 1979. A Non-Parametric Approach to the Change-Point Problem. J. R. Stat. Soc. Ser. C Appl. Stat. 28, 126–135. https://doi.org/10.2307/2346729

Quesada-Román, A., Ballesteros-Cánovas, J.A., St. George, S., Stoffel, M., 2022. Tropical and subtropical dendrochronology: Approaches, applications, and prospects. Ecol. Indic. 144, 109506. https://doi.org/10.1016/j.ecolind.2022.109506

Rao, M.P., Cook, E.R., Cook, B.I., Anchukaitis, K.J., D'Arrigo, R.D., Krusic, P.J., LeGrande, A.N., 2019. A double bootstrap approach to Superposed Epoch Analysis to evaluate response uncertainty. Dendrochronologia 55, 119–124. https://doi.org/10.1016/j.dendro.2019.05.001

Rasmusson, E.M., Carpenter, T.H., 1982. Variations in tropical sea surface temperature and surface wind fields associated with the Southern Oscillation/El Niño. Mon. Weather Rev. 110, 354–384.

Rehm, E.M., Feeley, K.J., 2013. Forest patches and the upward migration of timberline in the southern Peruvian Andes. For. Ecol. Manag. 305, 204–211. https://doi.org/10.1016/j.foreco.2013.05.041

Requena-Rojas, E.J., Amoroso, M.M., Ticse-Otarola, G., Crispin-Delacruz, D.B., 2021. Assessing Dendrochronological Potential of Escallonia myrtilloides in the High Andes of Peru. Tree-Ring Res. 77, 41–52. https://doi.org/10.3959/TRR2019-8

Requena-Rojas, E.J., Crispín-DelaCruz, D.B., Ticse-Otarola, G., Quispe-Melgar, H.R., Inga Guillen, J.G., Camel Paucar, V., Guerra, A., Ames-Martinez, F.N., Morales, M., 2020. Temporal Growth Variation in High-Elevation Forests: Case Study of Polylepis Forests in Central Andes, in: Pompa-García, M., Camarero, J.J. (Eds.), Latin American Dendroecology: Combining Tree-Ring Sciences and Ecology in a Megadiverse Territory. Springer International Publishing, Cham, pp. 263–279. https://doi.org/10.1007/978-3-030-36930-9_12

Roig, F., Fernández, M., Gareca León, E., Altamirano, S., Monge, S., 2001. ESTUDIOS DENDROCRONOLÓGICOS EN LOS AMBIENTES HÚMEDOS DE LA PUNA BOLIVIANA DENDROCHRONOLOGICAL STUDIES IN THE HUMID PUNA ENVIRONMENTS OF BOLIVIA. Rev Bol Ecol 9.

Rolland, C., Petitcolas, V., Michalet, R., 1998. Changes in radial tree growth for Picea abies, Larix decidua, Pinus cembra and Pinus uncinata near the alpine timberline since 1750. Trees 13, 40–53. https://doi.org/10.1007/PL00009736

Romatschke, U., Houze, R.A., 2010. Extreme Summer Convection in South America. https://doi.org/10.1175/2010JCLI3465.1

Ronchail, J., Espinoza, J.C., Drapeau, G., Sabot, M., Cochonneau, G., Schor, T., 2018. The flood recession period in Western Amazonia and its variability during the 1985–2015 period. J. Hydrol. Reg. Stud. 15, 16–30. https://doi.org/10.1016/j.ejrh.2017.11.008

Ropelewski, C.F., Halpert, M.S., 1987. Global and Regional Scale Precipitation Patterns Associated with the El Niño/Southern Oscillation.

Schulman, E., 1956. Dendroclimatic Changes in Semiarid America. University of Arizona Press, Tucson, p. 142.

Segura, H., Espinoza, J.C., Junquas, C., Lebel, T., Vuille, M., Condom, T., 2022. Extreme austral winter precipitation events over the South-American Altiplano: regional atmospheric features. Clim. Dyn. 59, 3069–3086. https://doi.org/10.1007/s00382-022-06240-1

Sierra, J.P., Junquas, C., Espinoza, J.C., Segura, H., Condom, T., Andrade, M., Molina-Carpio, J., Ticona, L., Mardoñez, V., Blacutt, L., Polcher, J., Rabatel, A., Sicart, J.E., 2022. Deforestation impacts on Amazon-Andes hydroclimatic connectivity. Clim. Dyn. 58, 2609–2636. https://doi.org/10.1007/s00382-021-06025-y

Simpson, B.B., 1979. A revision of the genus Polylepis (Rosaceae: Sanguisorbeae). Smithson. Contrib. Bot.

Smirnov, N., 1948. Table for estimating the goodness of fit of empirical distributions. Ann. Math. Stat. 19, 279–281.

Srur, A.M., Villalba, R., Rodríguez-Catón, M., Amoroso, M.M., Marcotti, E., 2018. Climate and Nothofagus pumilio Establishment at Upper Treelines in the Patagonian Andes. Front. Earth Sci. 6. https://doi.org/10.3389/feart.2018.00057

Srur, A.M., Villalba ,Ricardo, Rodríguez-Catón ,Milagros, Amoroso ,Mariano M., and Marcotti, E., 2016. Establishment of Nothofagus pumilio at Upper Treelines Across a Precipitation Gradient in the Northern Patagonian Andes. Arct. Antarct. Alp. Res. 48, 755–766. https://doi.org/10.1657/AAAR0016-015

Stokes, M.A., Smiley, T.L., 1968. An introduction to tree-ring dating. University of Chicago Press, Chicago, Illinois.

Thompson, L.G., Mosley-Thompson, E., Brecher, H., Davis, M., León, B., Les, D., Lin, P.-N., Mashiotta, T., Mountain, K., 2006. Abrupt tropical climate change: Past and present. Proc. Natl. Acad. Sci. 103, 10536–10543. https://doi.org/10.1073/pnas.0603900103

Tovar, C., Carril, A.F., Gutiérrez, A.G., Ahrends, A., Fita, L., Zaninelli, P., Flombaum, P., Abarzúa, A.M., Alarcón, D., Aschero, V., Báez, S., Barros, A., Carilla, J., Ferrero, M.E., Flantua, S.G.A., Gonzáles, P., Menéndez, C.G., Pérez-Escobar, O.A., Pauchard, A., Ruscica, R.C., Särkinen, T., Sörensson, A.A., Srur, A., Villalba, R., Hollingsworth, P.M., 2022. Understanding climate change impacts on biome and plant distributions in the Andes: Challenges and opportunities. J. Biogeogr. 49, 1420–1442. https://doi.org/10.1111/jbi.14389

Vera, C., Higgins, W., Amador, J., Ambrizzi, T., Garreaud, R., Gochis, D., Gutzler, D., Lettenmaier, D., Marengo, J., Mechoso, C.R., Nogues-Paegle, J., Silva Dias, P.L., Zhang, C., 2006. Toward a Unified View of the American Monsoon Systems. J. Clim. 19, 4977–5000. https://doi.org/10.1175/JCLI3896.1

Virtanen, P., Gommers, R., Oliphant, T.E., Haberland, M., Reddy, T., Cournapeau, D., Burovski, E., Peterson, P., Weckesser, W., Bright, J., 2020. SciPy 1.0: fundamental algorithms for scientific computing in Python. Nat. Methods 17, 261–272.

von Arx, G., Crivellaro, A., Prendin, A.L., Čufar, K., Carrer, M., 2016. Quantitative Wood Anatomy—Practical Guidelines. Front. Plant Sci. 7.

Vuille, M., Bradley, R.S., Keimig, F., 2000. Interannual climate variability in the Central Andes and its relation to tropical Pacific and Atlantic forcing. J. Geophys. Res. Atmospheres 105, 12447–12460. https://doi.org/10.1029/2000JD900134

Waskom, M.L., 2021. seaborn: statistical data visualization. J. Open Source Softw. 6, 3021. https://doi.org/10.21105/joss.03021

Wigley, T.M.L., Briffa, K.R., Jones, P.D., 1984. On the Average Value of Correlated Time Series, with Applications in Dendroclimatology and Hydrometeorology. J. Appl. Meteorol. Climatol. 23, 201–213. https://doi.org/10.1175/1520-0450(1984)023<0201:OTAVOC>2.0.CO;2

Wilmking, M., D'Arrigo, R., Jacoby, G.C., Juday, G.P., 2005. Increased temperature sensitivity and divergent growth trends in circumpolar boreal forests. Geophys. Res. Lett. 32. https://doi.org/10.1029/2005GL023331

Wolter, K., Timlin, M.S., 2011. El Niño/Southern Oscillation behaviour since 1871 as diagnosed in an extended multivariate ENSO index (MEI.ext). Int. J. Climatol. 31, 1074–1087. https://doi.org/10.1002/joc.2336

Yoon, J., Zeng, N., 2010. An Atlantic influence on Amazon rainfall. Clim. Dyn. 34, 249–264. https://doi.org/10.1007/s00382-009-0551-6

Young, K.R., León, B., 2006. Tree-line changes along the Andes: implications of spatial patterns and dynamics. Philos. Trans. R. Soc. B Biol. Sci. 362, 263–272. https://doi.org/10.1098/rstb.2006.1986

Zang, C., Biondi, F., 2015. treeclim: an R package for the numerical calibration of proxy-climate relationships. Ecography 38, 431–436. https://doi.org/10.1111/ecog.01335

Zanin, P.R., Satyamurty, P., 2020. Hydrological processes interconnecting the two largest watersheds of South America from multi-decadal to inter-annual time scales: A critical review. Int. J. Climatol. 40, 4006–4038. https://doi.org/10.1002/joc.6442

Zapata, F., 2013. A multilocus phylogenetic analysis of Escallonia (Escalloniaceae): Diversification in montane South America. Am. J. Bot. 100, 526–545. https://doi.org/10.3732/ajb.1200297